BTE-Barna: first-principles thermal simulation of devices based on 2D materials

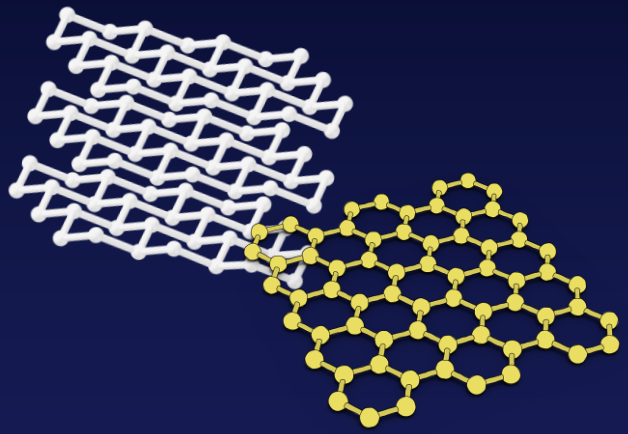

Authors:
Martí Raya-Moreno
Xavier Cartoixà
Jesús Carrete

14th June 2023

UAB Universitat Autònoma de Barcelona
TU WIEN TECHNISCHE UNIVERSITÄT WIEN
ICMAB INSTITUT DE CIÈNCIA DE MATERIALS DE BARCELONA
EXCELENCIA SEVERO OCHOA
CSIC CONSEJO SUPERIOR DE INVESTIGACIONES CIENTÍFICAS

Outline

1. Introduction
2. BTE-Barna: the solvers
3. BTE-Barna: examples
4. Real case: Hydrodynamic signatures in 2D devices.
5. Conclusions
6. Acknowledgements

Introduction

Why heat transport?

- Thermal waste is a serious issue in transistors

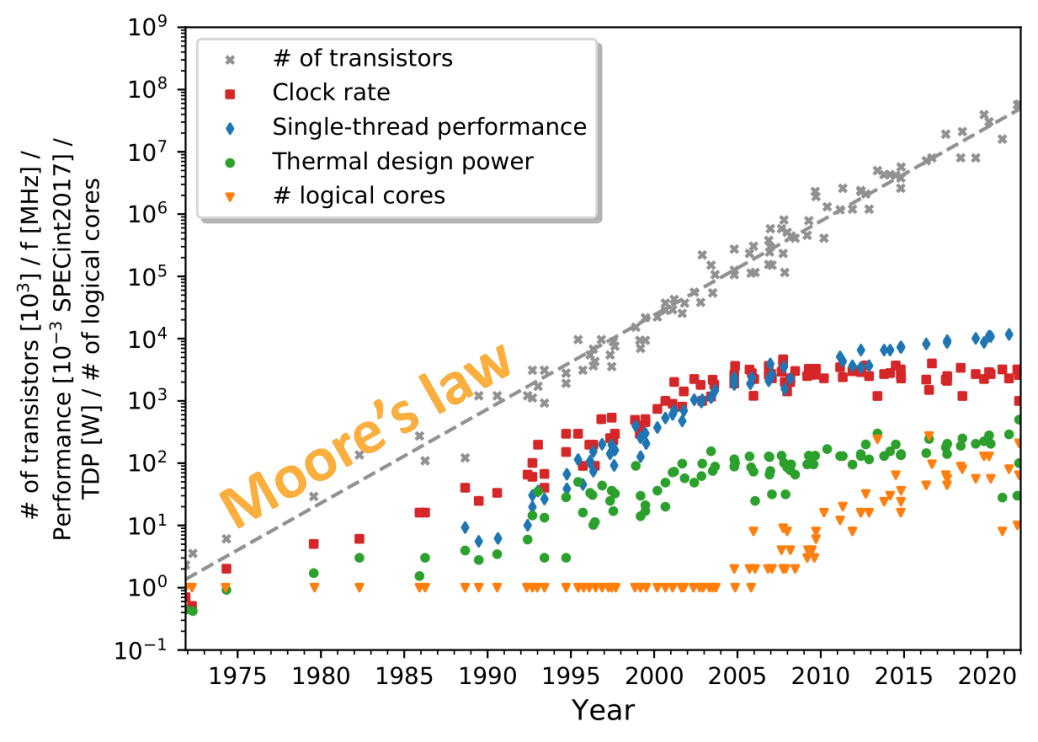

Processors characteristics per release year. Data has been collected by Rupp (https://github.com/karlrupp/microprocessor-trend-data).

Why heat transport?

- Thermal waste is a serious issue in transistors

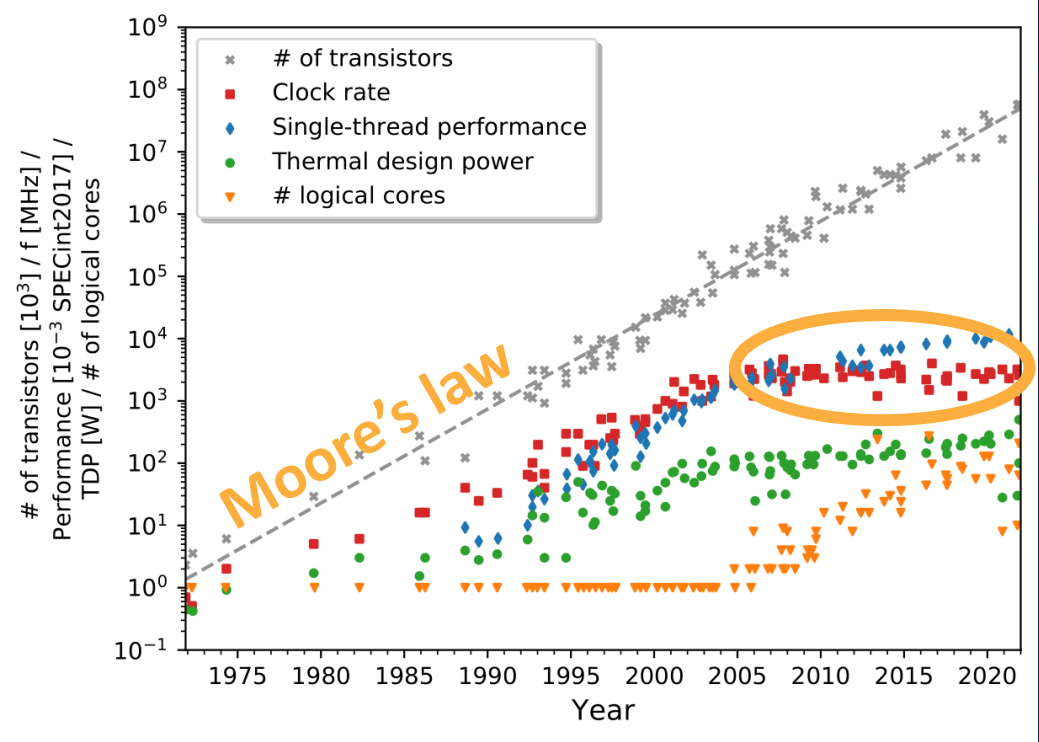

Clock-rate stagnation

Processors characteristics per release year. Data has been collected by Rupp (https://github.com/karlrupp/microprocessor-trend-data).

Why 2D materials?

- Moore's law exhaustion: We are arriving at atom level

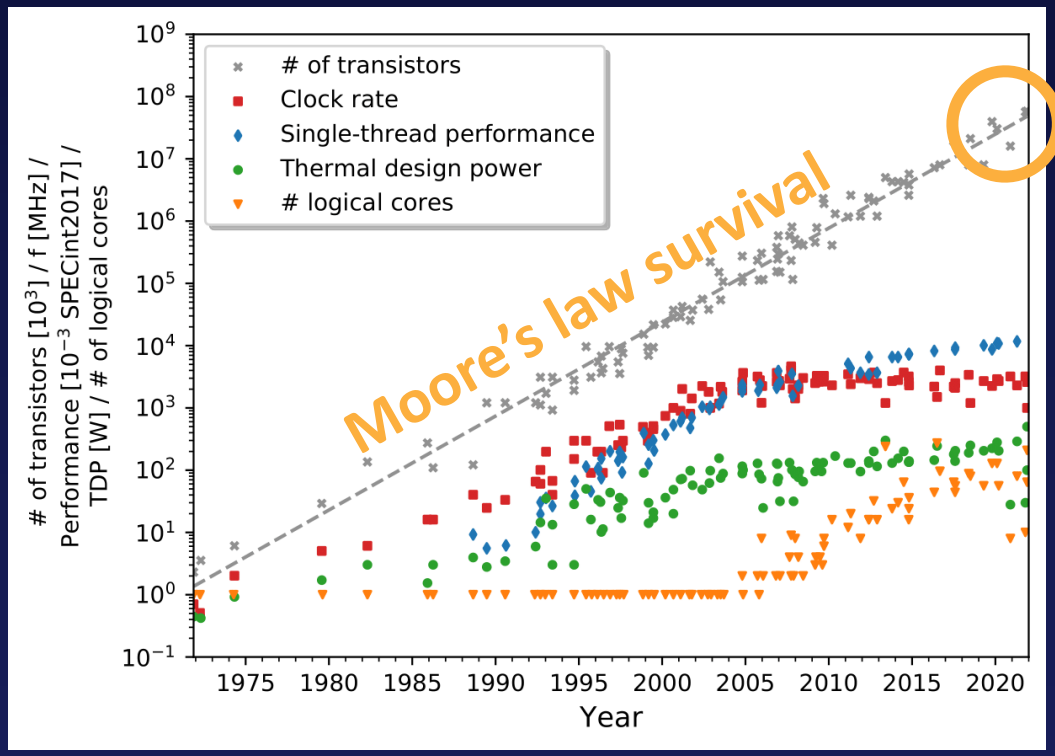

Physical limits i.e. atomic size

Processors characteristics per release year. Data has been collected by Rupp (https://github.com/karlrupp/microprocessor-trend-data).

Why heat ? Why 2D materials?

- Moore's law exhaustion: We are arriving at atom level

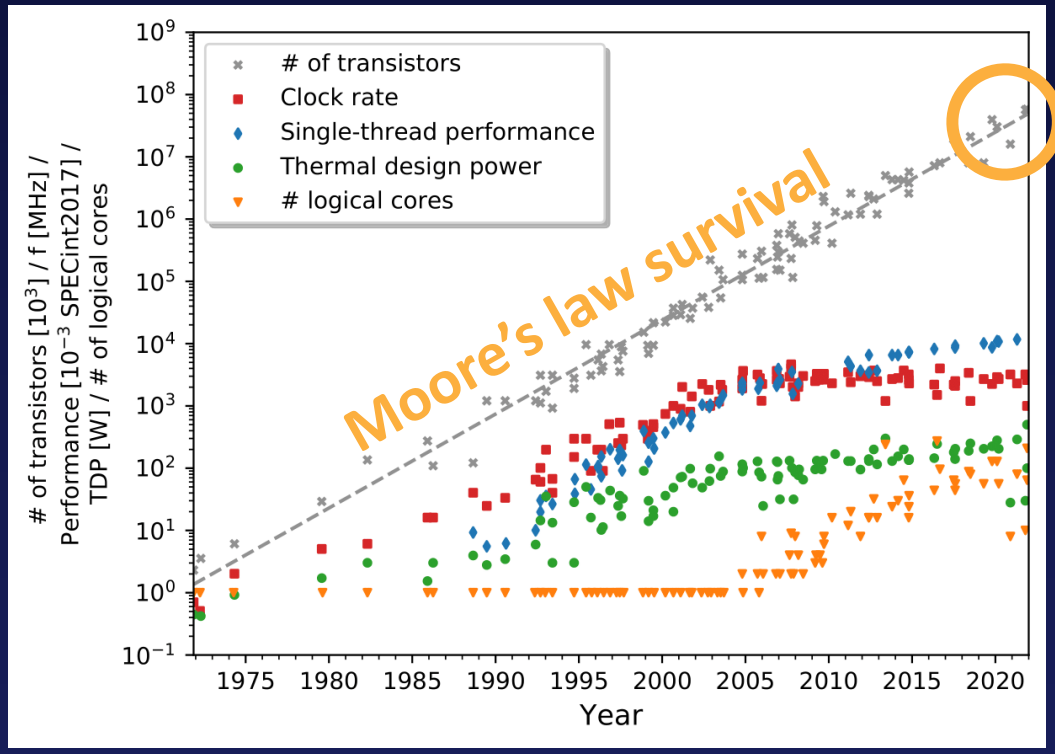

Physical limits i.e. atomic size

2D Materials

✓ Excellent physical properties
✓ Tunable properties through stacking
✓ CMOS compatible

Processors characteristics per release year. Data has been collected by Rupp (https://github.com/karlrupp/microprocessor-trend-data).

How do we model heat transport?

How do we model heat transport?

- Crystalline semiconductor/insulator: heat carried by bunches of phonons.

How do we model heat transport?

- Crystalline semiconductor/insulator: heat carried by bunches of phonons.

- The (linearized) Peierls-Boltzmann Transport equation (LPBTE):

$$\frac{\partial n_i^d}{\partial t} + \mathbf{v}_i \cdot \nabla n_i^d + \frac{\partial n_i^0}{\partial T} \mathbf{v}_i \cdot \nabla T_{\text{ref}} = \sum_j A_{ij} n_j^d$$

Practical solution for “complex” systems: almaBTE

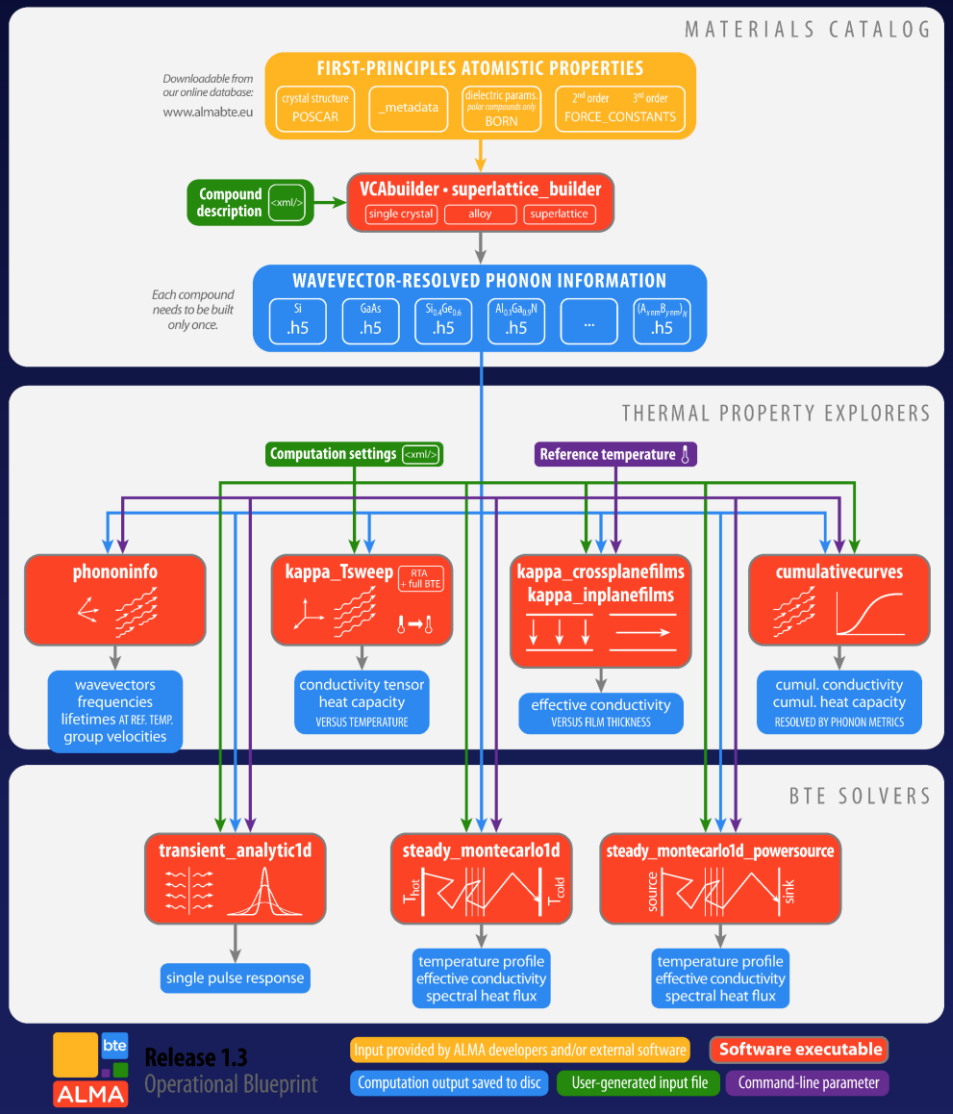

✓ First-principles based, no fitting.

✓ Works for relative complex structures/systems (alloys, superlattices, sandwiched heterostructures).

✓ Not based on oldish arbitrary concepts (N-U, L-T,..) but the RTA and beyond-RTA LPBTE.

General structure almaBTE version 1.3. Reproduced from https://almabte.bitbucket.io. Adapted from J. Carrete et. al. Comput. Phys. Commun. 220, 351 (2017).

Practical solution for “complex” systems: almaBTE

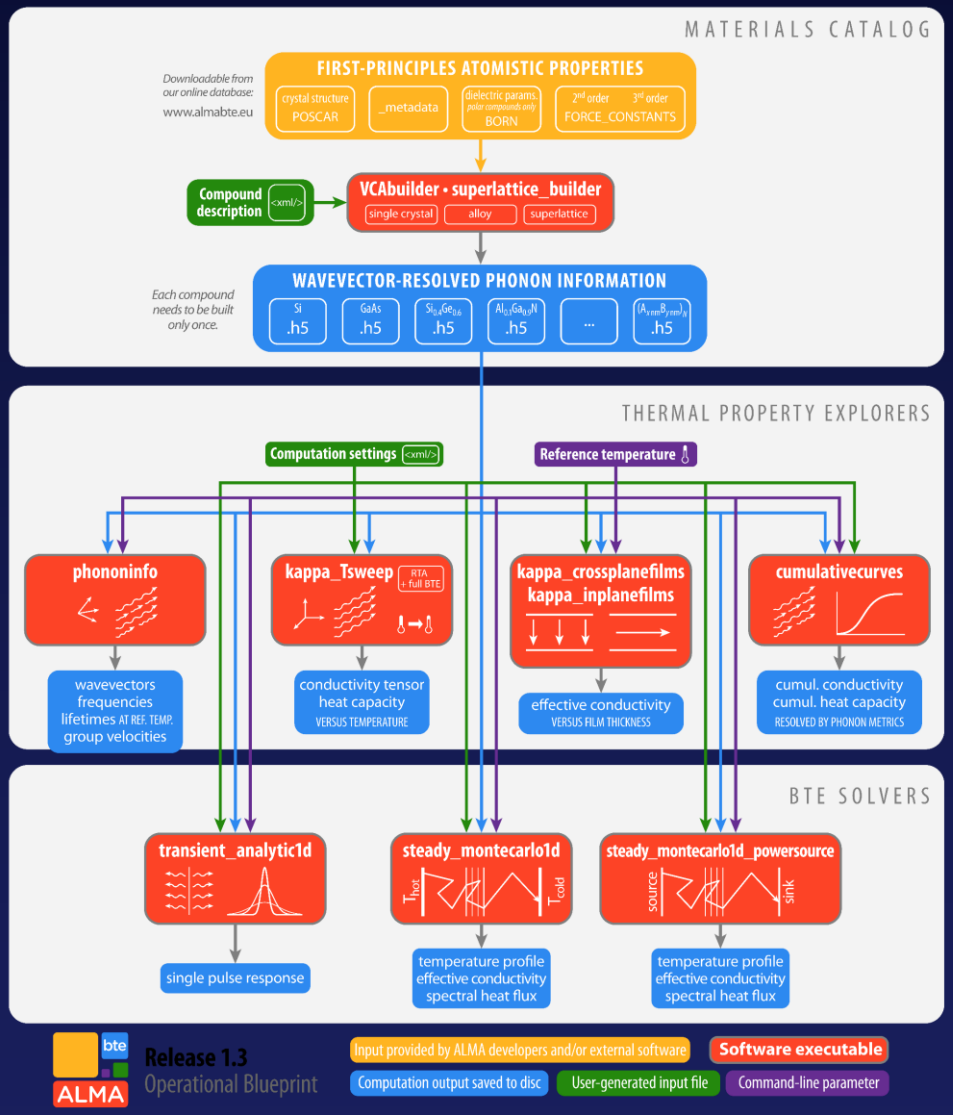

✗ κ_{eff} for nanowires (ShengBTE does) and nanoribbons are not implemented.

✗ MC is limited to simple steady-state sandwiched structures and uses the RTA (i.e. not valid for 2D systems, low T…)

General structure almaBTE version 1.3. Reproduced from https://almabte.bitbucket.io. Adapted from J. Carrete et. al. Comput. Phys. Commun. 220, 351 (2017).

BTE-Barna: the solvers

Solving limitations: BTE-Barna

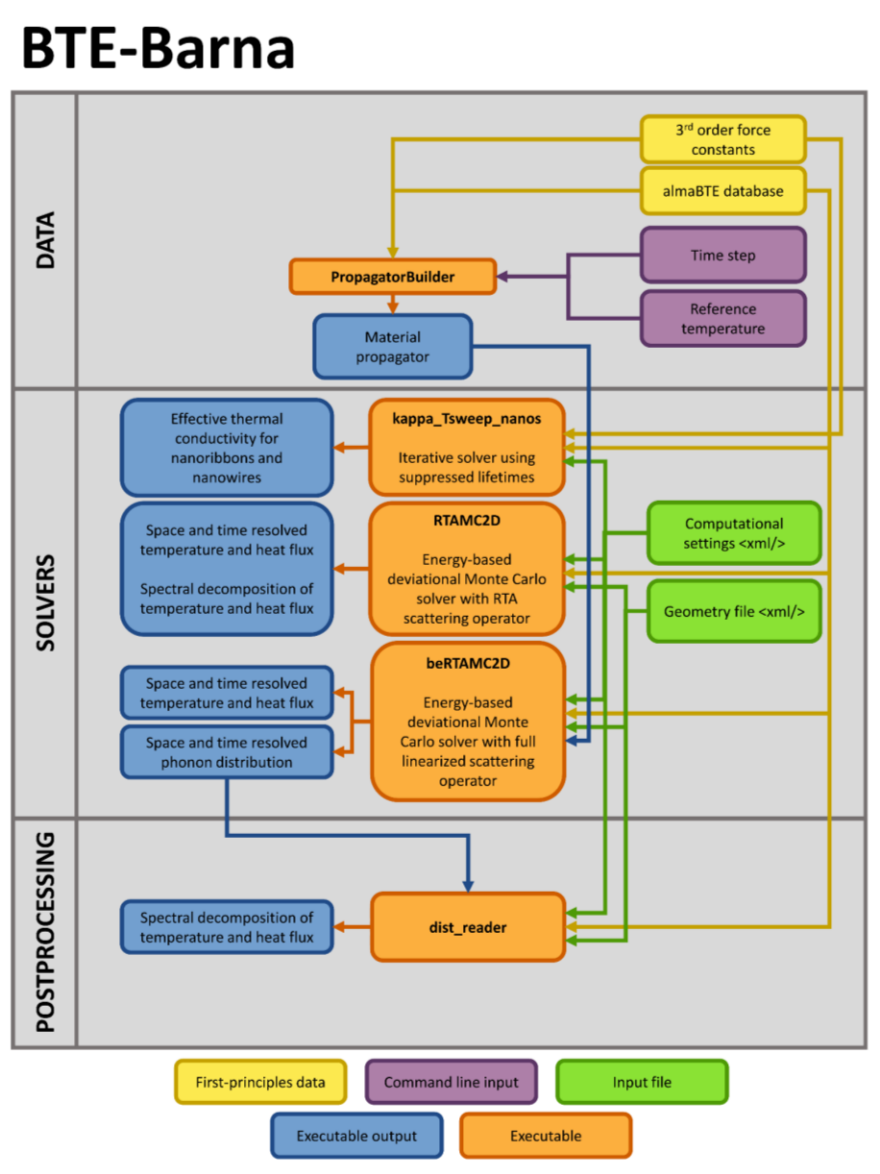

✓ κ_{eff} for nanowires and nanoribbons.

✓ MC is extended for 2D materials-based general geometries and initial conditions. It implements a full linearized approach to the scattering operator.

General structure of BTE-Barna package. Reproduced from M. Raya-Moreno *et al.* Comput. Phys. Commun **281,** 108504 (2022).

Solving limitations: BTE-Barna kappa_Tsweep_nanos

Iterative solver for nanoribbons and nanowires:

Go beyond homogeneous

$$\mathbf{v}_i \cdot \nabla n_i^d(\mathbf{r}) + \frac{\partial n_i^0}{\partial T}\mathbf{v}_i \cdot \nabla T = \sum_j A_{ij} n_j^{d(\mathbf{r})}$$

Average beyond the RTA effects and BC

$$n_i^d(\mathbf{r}) = \tau_i \left[-\frac{\partial n_i^0}{\partial T}\mathbf{v}_i \cdot \nabla T + \sum_{j \neq i} A_{ij} \bar{n}_j^d \right] \left[1 - \exp\left(-\frac{|\mathbf{r} - \mathbf{r}_B|}{\tau_i \mathbf{v}_B} \right) \right]$$

Average over the cross-section

$$\bar{n}_i^d = \tau_i^{\text{nano}} \left[-\frac{\partial n_i^0}{\partial T}\mathbf{v}_i \cdot \nabla T + \sum_{j \neq i} A_{ij} \bar{n}_j^d \right]$$

$$\tau_i^{\text{nano}} = \tau_i \frac{1}{A_C} \int_{A_c} 1 - \exp\left(-\frac{|\mathbf{r} - \mathbf{r}_B|}{\tau_i \mathbf{v}_B} \right) dS$$

✓ Bulk-like iterative expression

CM breakdown: Z. Wang and N. Mingo, Appl. Phys. Lett. **99**, 101903 (2011).
Theory: W. Li et al., Phys. Rev. B **85**, 195436 (2012).

BTE-Barna: RTA Monte Carlo (RTAMC2D)

Extends steady_montecarlo1d: Power deviational RTA Monte Carlo [1,2]

✗ It fails to describe 2D, finite systems and/or periodic systems.

Implemented diffusive boundary conditions (Lambert's cosine law) and PBC.

✗ Only 2 isothermal reservoirs as inputs

Added gradient initial conditions, and multiple reservoirs.

✗ No transient simulations

Added transient to the steady-state

✗ No simulations for periodic systems with an applied thermal gradient

Implemented specialized algorithm [1,3,4] for extended systems with applied gradients.

✗ DMM can couple unconnected layers for layered/sandwiched materials/systems leading to negative interface thermal resistance [5]

Implemented new model (localized DMM) for interface scattering based on DMM but accounting for mode localization in each layer for the mode coupling.

almaBTE
THERMAL SIMULATION

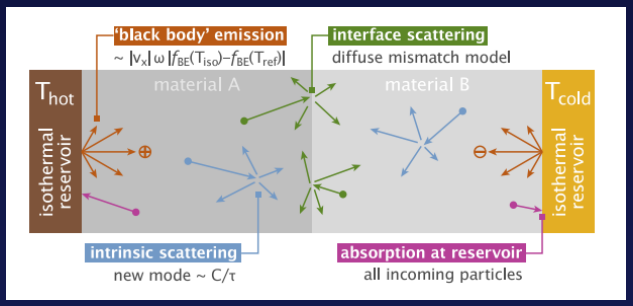

Schematic overview of possible events encountered by deviational particles in Monte Carlo simulations. Reproduced from J. Carrete et. al. Comput. Phys. Commun. 220, 351 (2017).

[1] J.-P. M. Péraud, et al., Annu. Rev. Heat Transf. 17, 205-265 (2014).
[2] J.-P. M. Péraud et al., Appl. Phys. Lett. 101, 153114 (2012).
[3] J. Randrianalisoa et al., J. Appl. Phys. 103, 053502 (2008).
[4] J. Randrianalisoa et al., J. Heat Transf. 130, 072404 (2008).
[5] M. Raya-Moreno *et al.* Comput. Phys. Commun. **281,** 108504 (2022).

BTE-Barna: RTA Monte Carlo (beRTAMC2D)

Going beyond RTA:

Deviational simulation of phonon transport in graphene ribbons with *ab initio* scattering

Cite as: J. Appl. Phys. **116**, 163502 (2014); https://doi.org/10.1063/1.4898090
Submitted: 17 April 2014 . Accepted: 02 October 2014 . Published Online: 22 October 2014

Colin D. Landon, and Nicolas G. Hadjiconstantinou

- Energy-deviational (natural E-conservation in scattering).
- Scattering modeled through the applying of the propagator:

$$n^d(t + \Delta t) = e^{\mathrm{B}\Delta t}\, n^d(t)$$

- Complexity comes from exponential of the collision matrix (complex task, efficiently solved using the Krylov subspace method):

BTE-Barna: examples

Monte Carlo codes: Phosphorene nanoribbons (AC; 300 K)

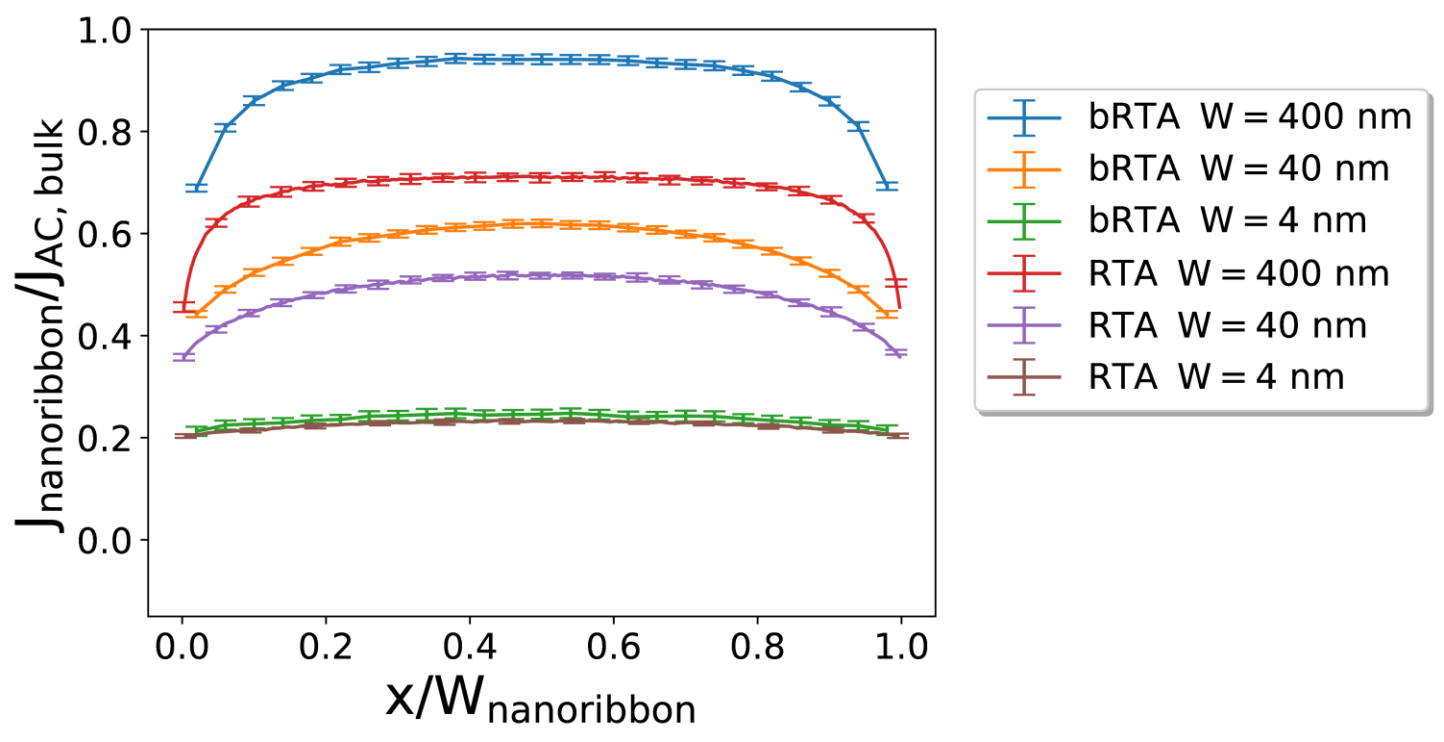

RTA and bRTA bulk-normalized heat flux in the AC direction as a function of the normalized position for a phosphorene nanoribbon with ∇T_{AC} = 0.2K/nm. Reproduced from M. Raya-Moreno *et al.* Comput. Phys. Commun. **281,** 108504 (2022).

Monte Carlo codes: Phosphorene nanoribbons (AC; 300 K)

Fitting (κ and ℓ) to hydrodynamic equation based on [A. Sellito et al., Proc. R. Soc. A: Math. Phys. Eng. Sci. 471, 20150376 (2015)].

$$J(x) = -\kappa \left\{ 1 - \frac{1}{1 - 2\tanh\left(\frac{W}{2\ell}\right)} \frac{\cosh\left(\frac{x}{\ell}\right)}{\cosh\left(\frac{W}{2\ell}\right)} \right\} \nabla T$$

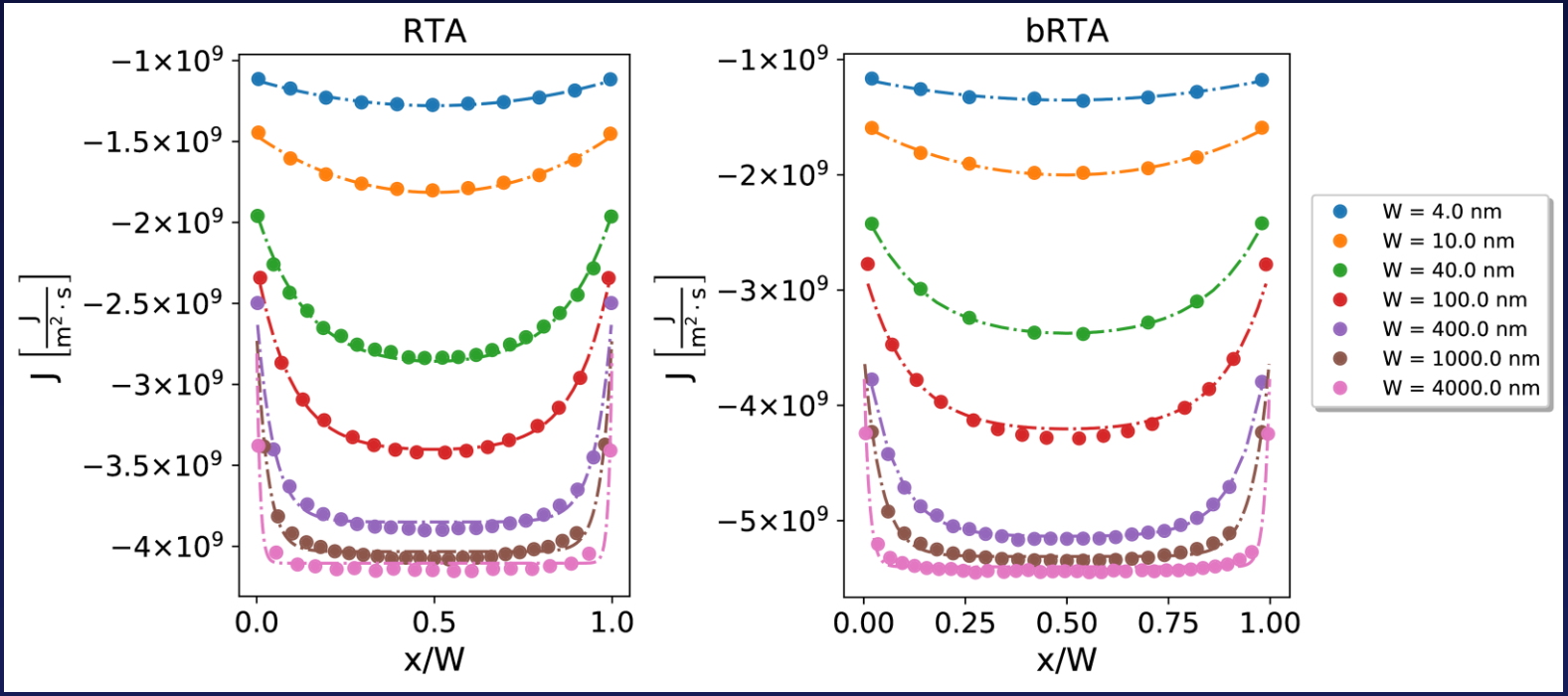

Fitting to hydrodynamic equation (lines) of RTA-MC (left) and bRTA-MC (right) calculated heat flux (points) as a function of normalized position for phosphorene AC nanoribbons of different widths under the effect of ∇T_{AC} = 0.2K/nm. Reproduced from M. Raya-Moreno *et al.* Comput. Phys. Commun. **281,** 108504 (2022).

Monte Carlo codes: Phosphorene nanoribbons (AC; 300 K)

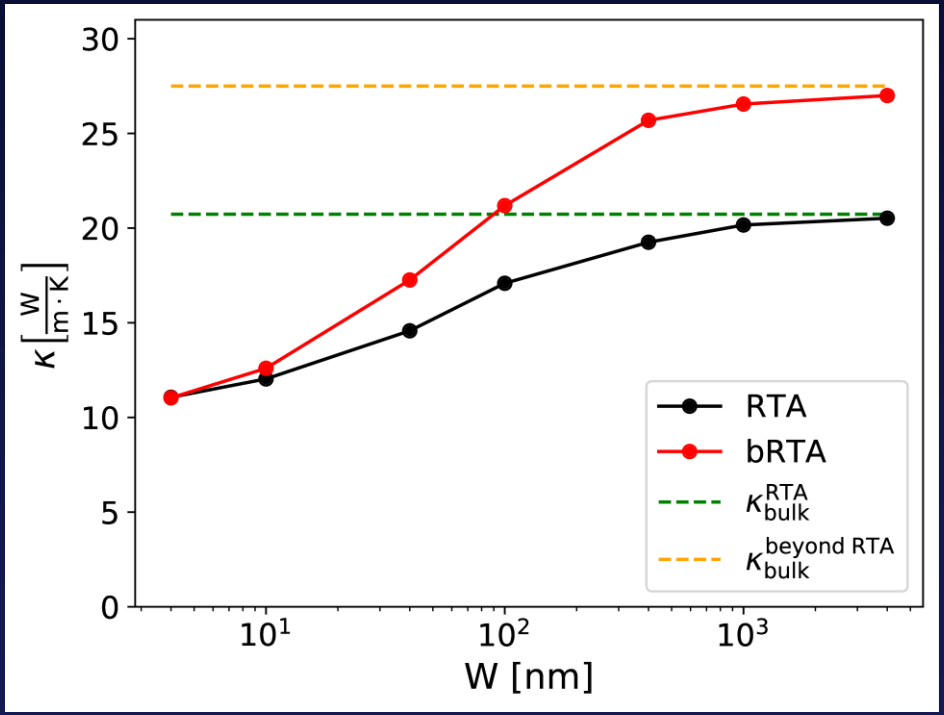

Fitted thermal conductivity as a function of AC nanoribbon width. Reproduced from M. Raya-Moreno *et al.* Comput. Phys. Commun. **281,** 108504 (2022).

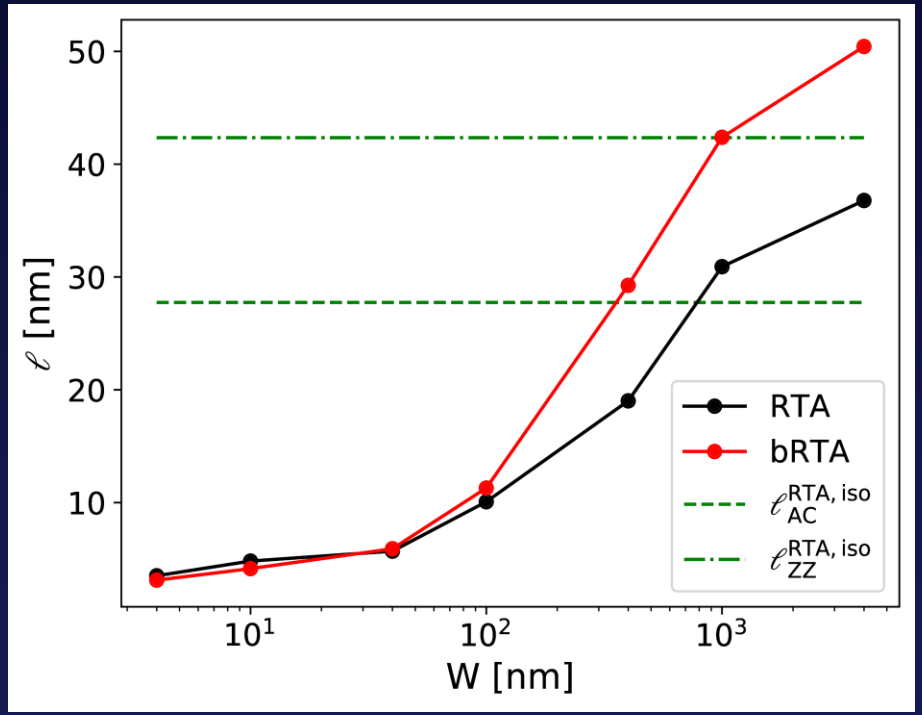

Fitted non-local distance ℓ as a function of AC nanoribbon width. Reproduced from M. Raya-Moreno *et al.* Comput. Phys. Commun. **281,** 108504 (2022).

Suppressed iterative solver: Phosphorene nanoribbons

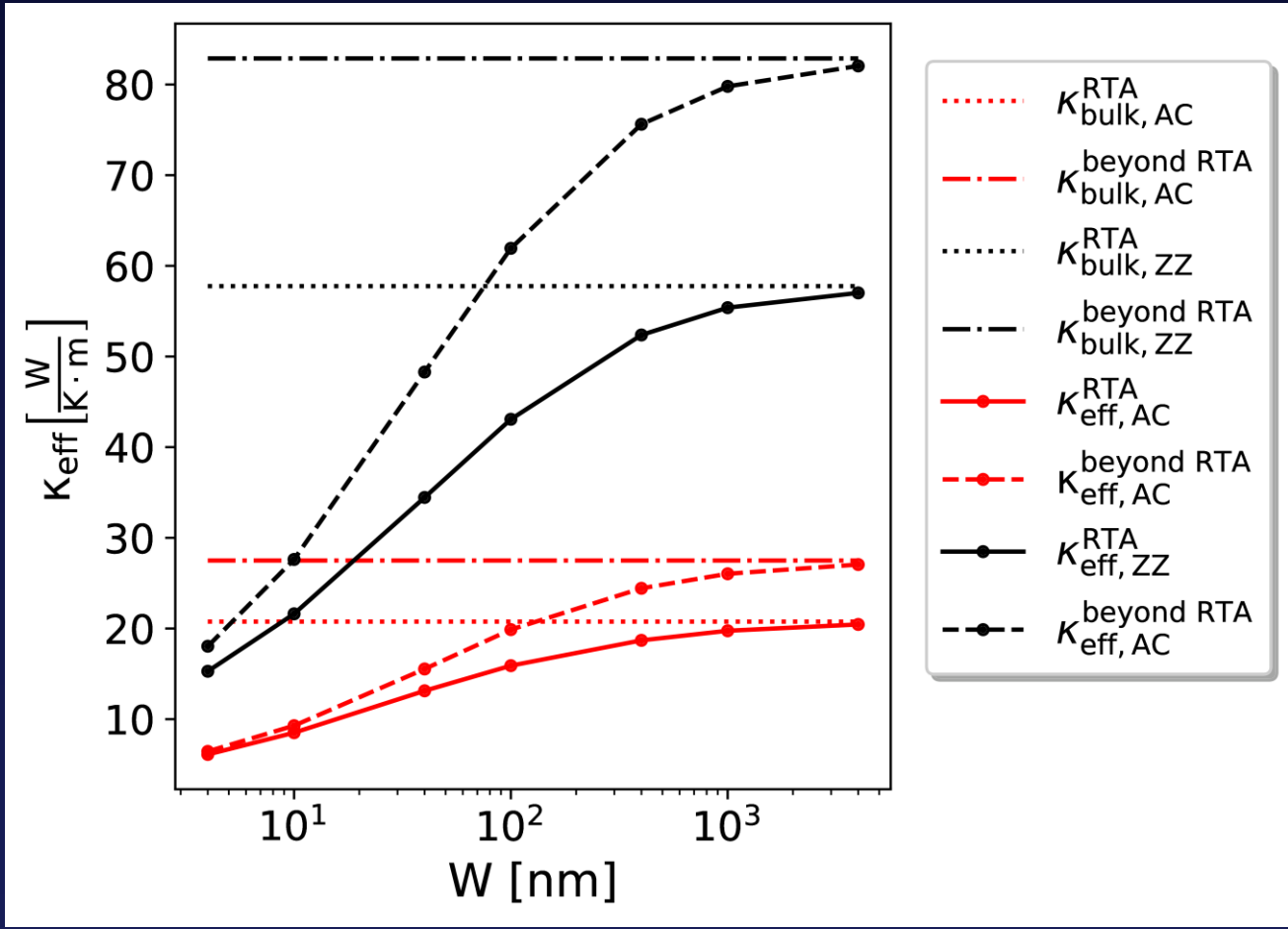

Effective thermal conductivity for AC and ZZ phosphorene nanoribbons for different widths. Reproduced from M. Raya-Moreno et al. Comput. Phys. Commun. 281, 108504 (2022).

Time dependent problems

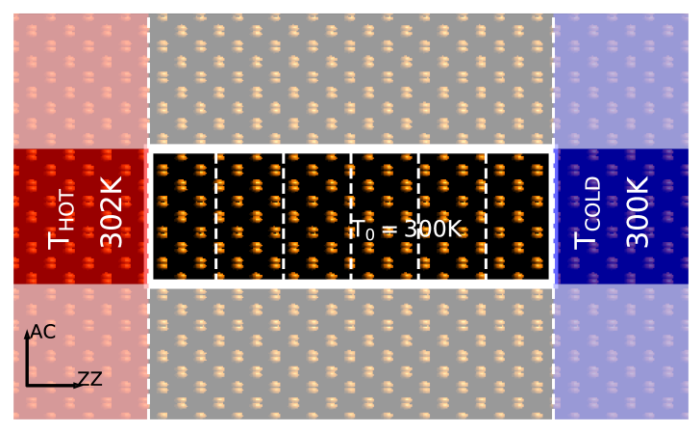

Sketch of phosphorene heating simulation in ZZ direction. Periodic boundary conditions are depicted with off-color boxes. Reproduced from M. Raya-Moreno et al. Comput. Phys. Commun. 281, 108504 (2022).

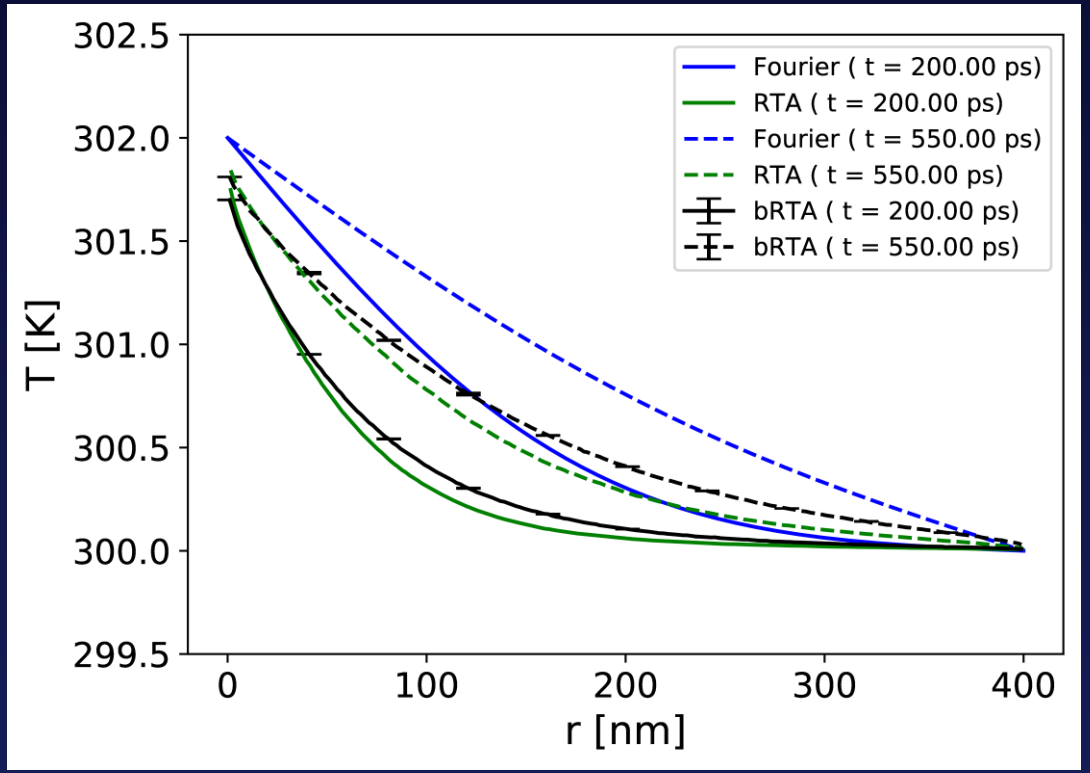

Temperature profiles obtained at different times using RTA-MC, bRTA-MC and Fourier. Reproduced from M. Raya-Moreno et al. Comput. Phys. Commun. 281, 108504 (2022).

MC solvers: Spectral decompostions (heating system)

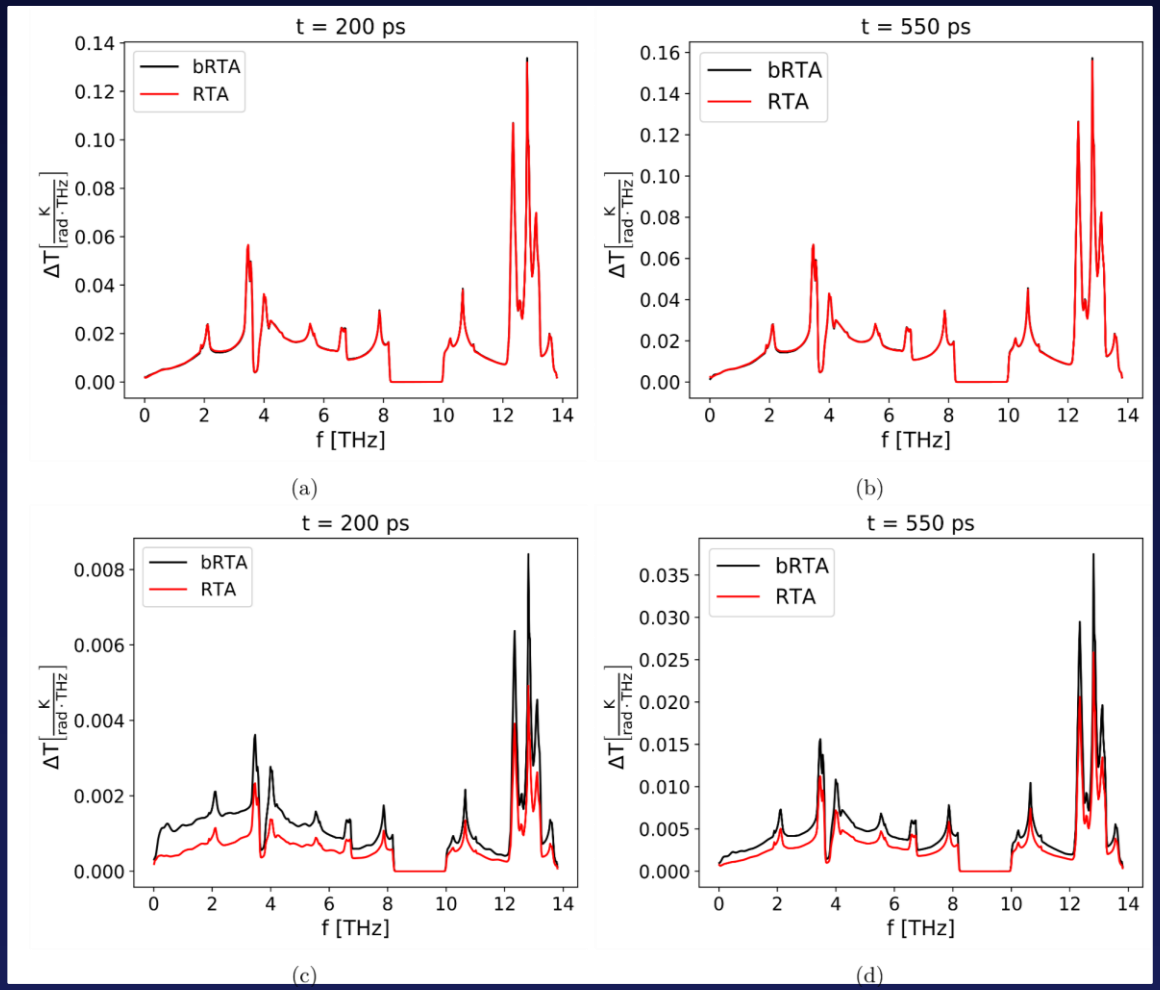

Spectral decomposition of deviational temperature at different times and positions. Reproduced from M. Raya-Moreno et al. Comput. Phys. Commun. 281, 108504 (2022).

Complex devices: wedge-like structure

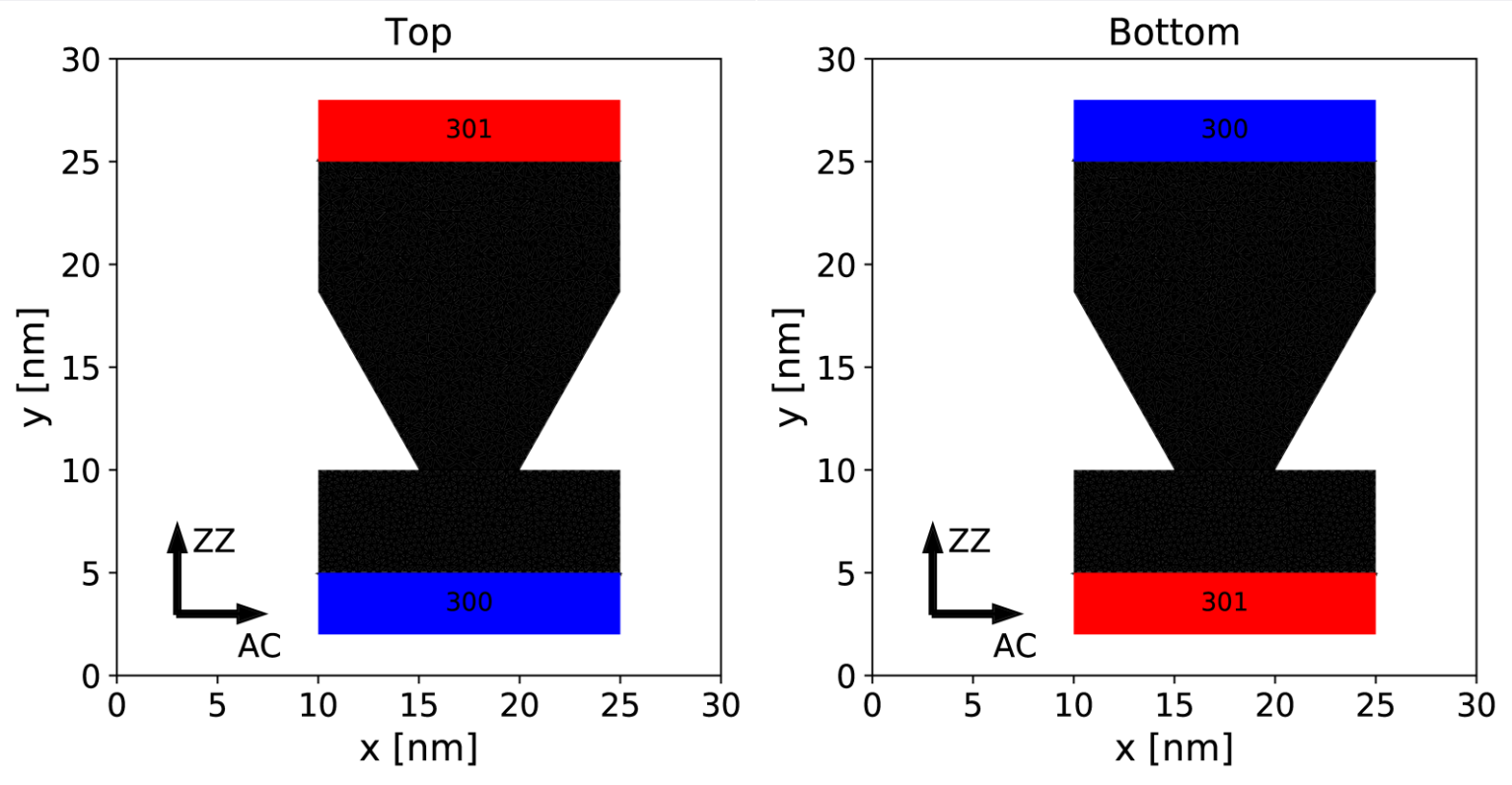

Phosphorene wedge-like geometry with hot reservoir at the top or at the bottom. Reproduced from M. Raya-Moreno et al. Comput. Phys. Commun. 281, 108504 (2022).

Complex devices: wedge-like structure

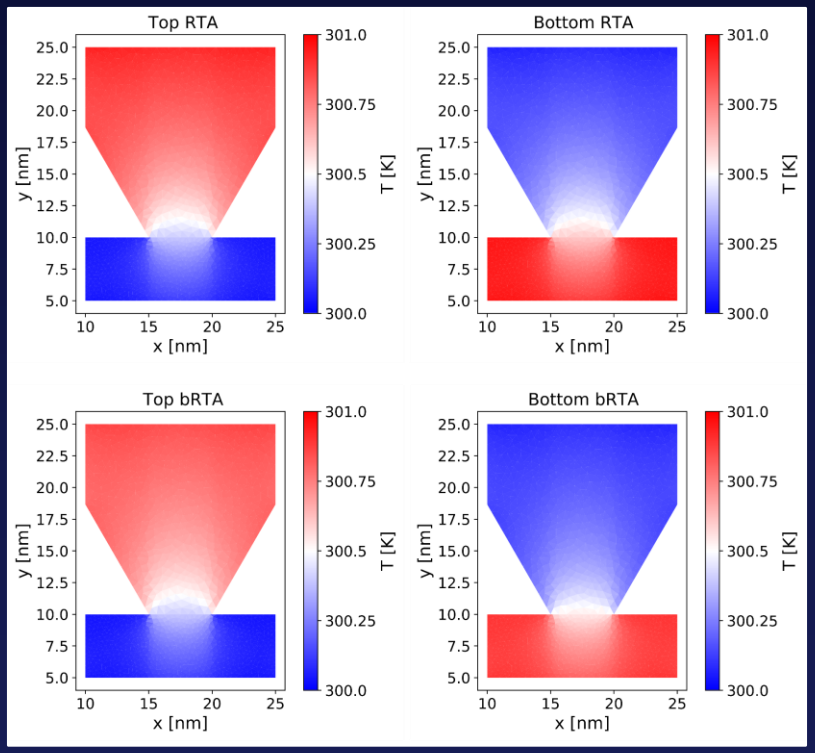

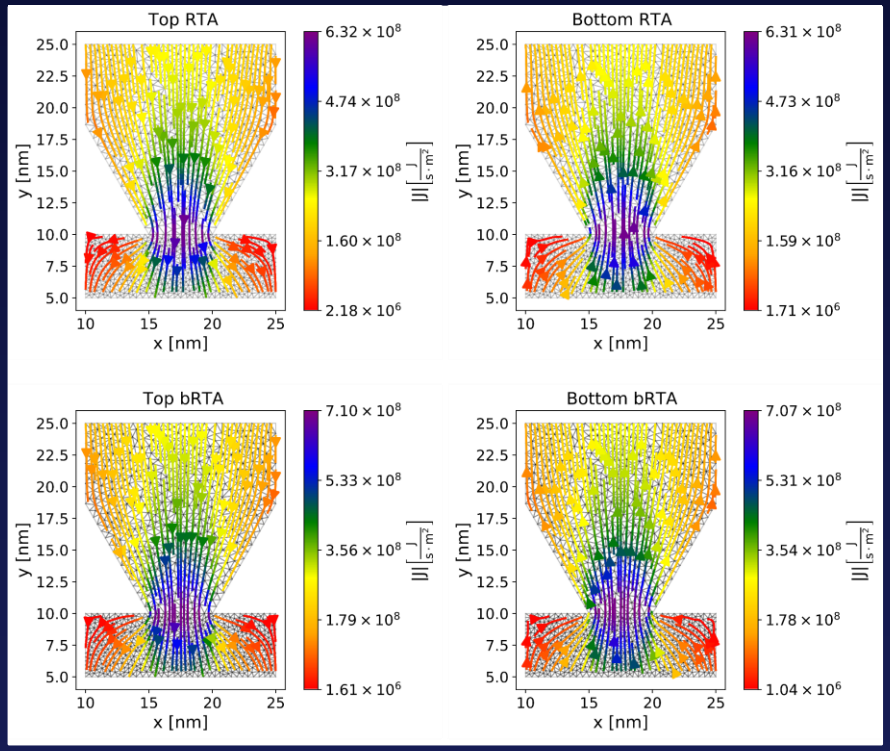

RTA and beyond RTA temperature profiles (left) and steady-state heat fluxes for wedge-like configurations at steady-state. Reproduced from M. Raya-Moreno et al. Comput. Phys. Commun. 281, 108504 (2022).

Complex devices: wedge-like structure

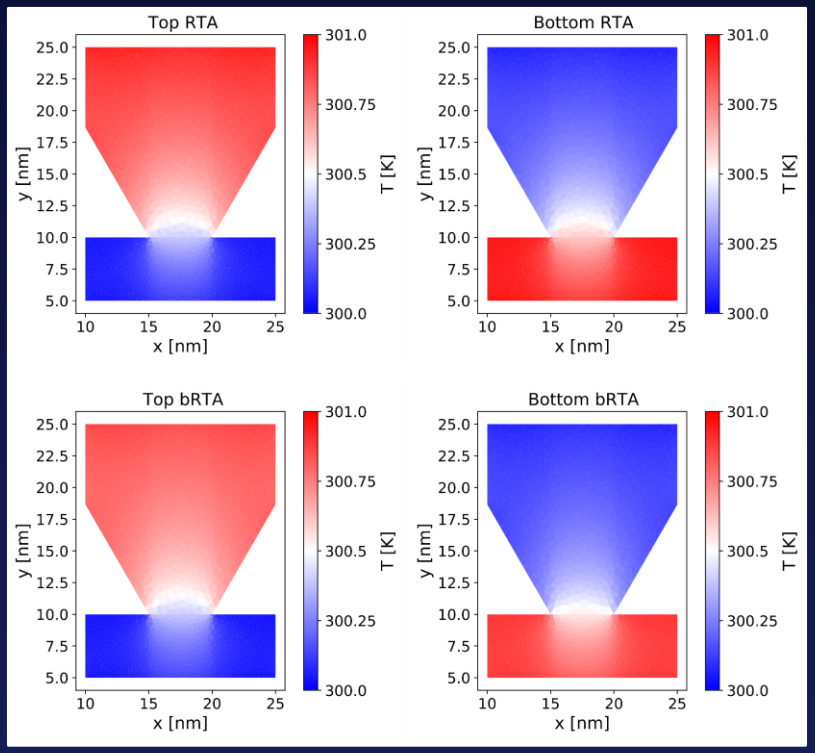

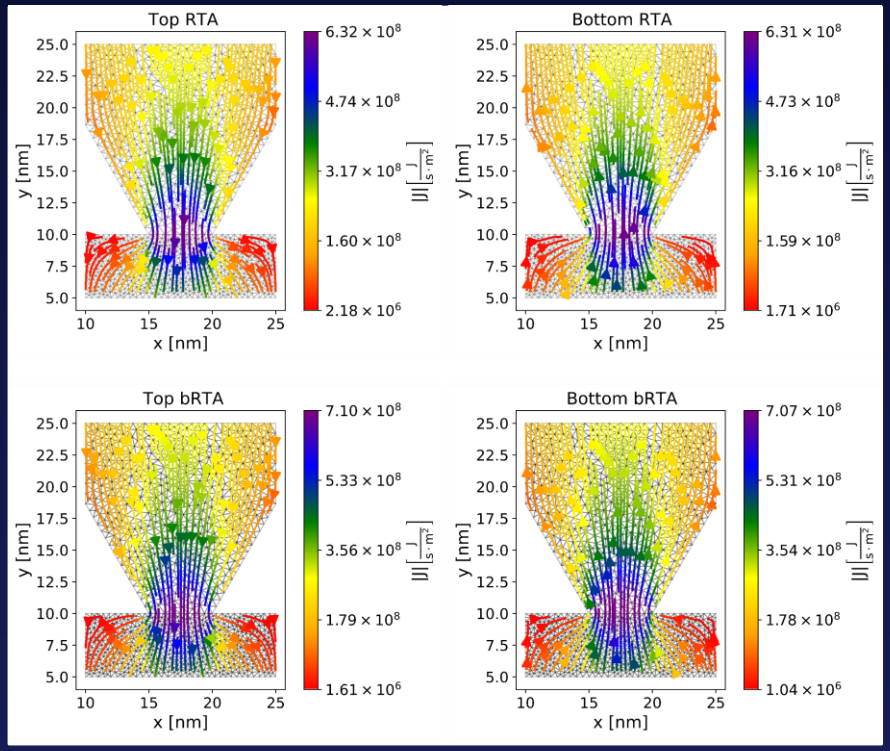

RTA and beyond RTA temperature profiles (left) and steady-state heat fluxes for wedge-like configurations at steady-state. Reproduced from M. Raya-Moreno et al. Comput. Phys. Commun. 281, 108504 (2022).

✗ No rectification (no confinement effects, small temperature bias,…)

Multiterminal devices

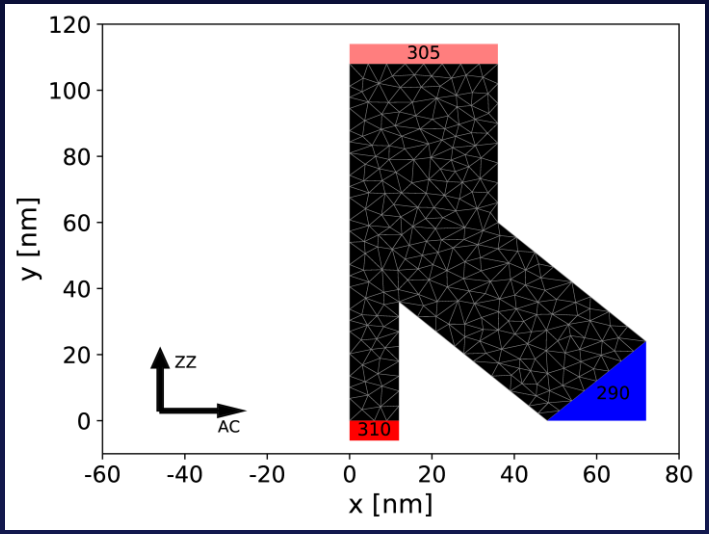

Example phosphorene structure with multiple terminals (isothermal reservoirs) at 310K, 305K and 290K. Reproduced from M. Raya-Moreno et al. Comput. Phys. Commun. 281, 108504 (2022).

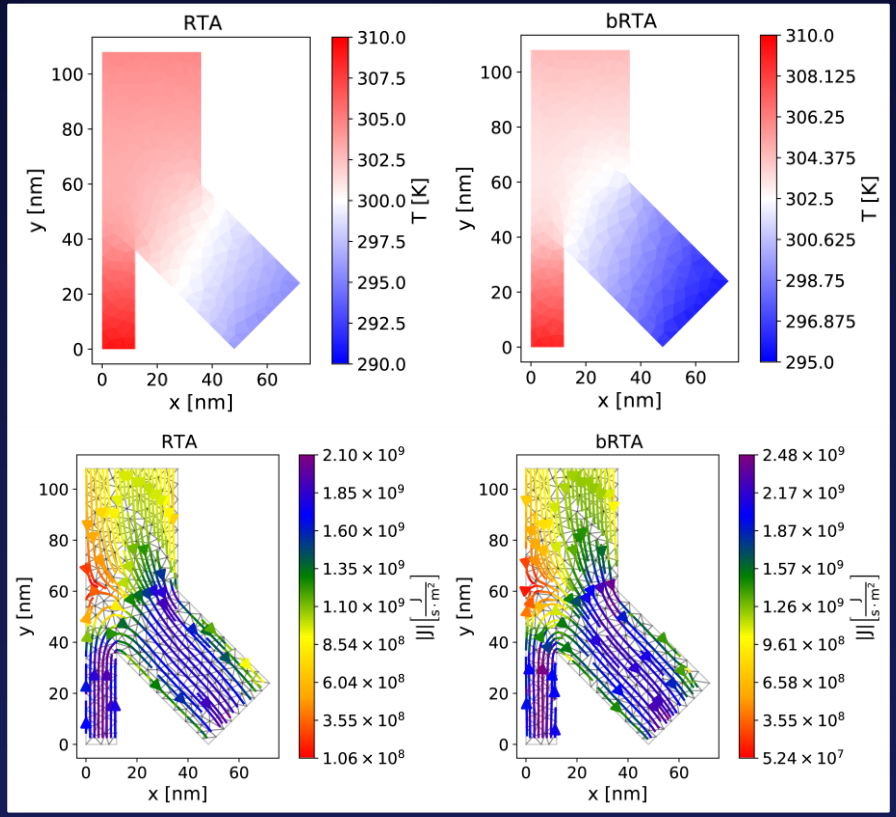

Steady-state thermal profiles and heat fluxes for the multiterminal structure. Reproduced from M. Raya-Moreno et al. Comput. Phys. Commun. 281, 108504 (2022).

Devices with interfaces (RTAMC2D-only)

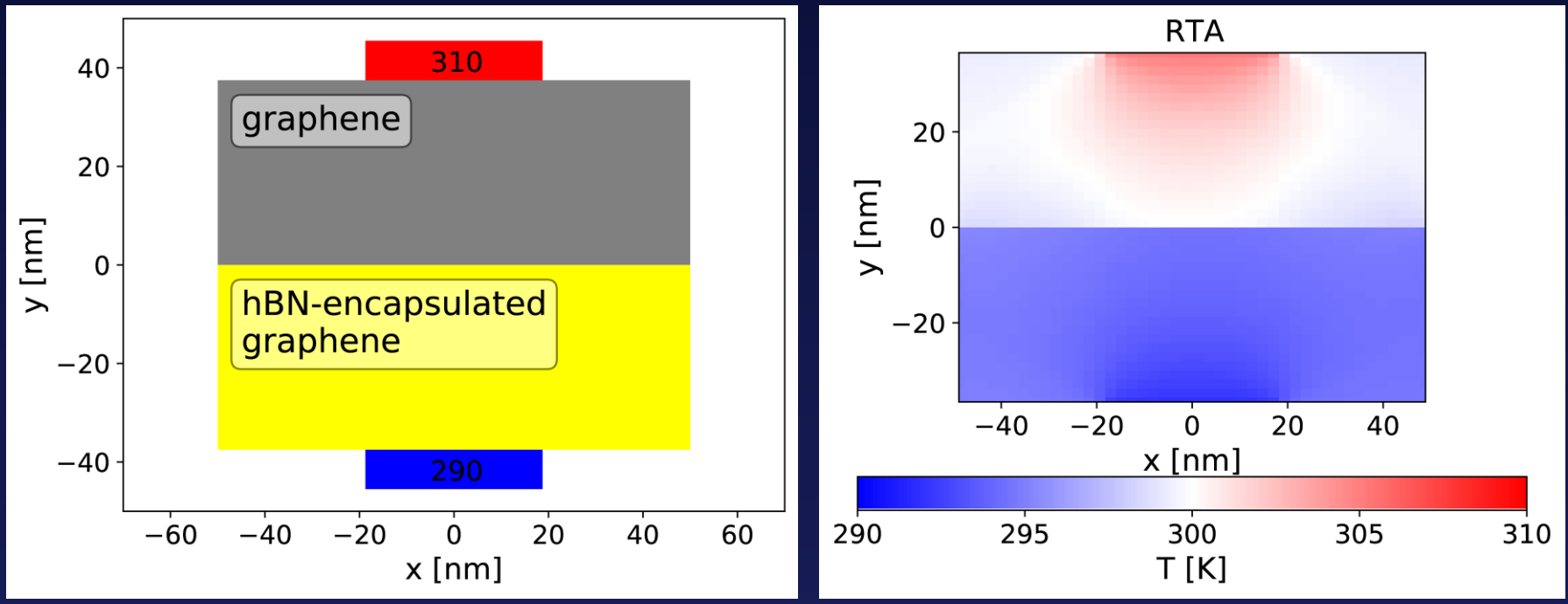

Sketch of structure with interface and its thermal profile. Reproduced from M. Raya-Moreno et al. Comput. Phys. Commun. 281, 108504 (2022).

Real problem: Hydrodynamic signatures in 2D devices

[M. Raya-Moreno et al., Phys. Rev. B 106, 014308 (2022).]

Levitov configuration and hydrodynamic signatures

- Levitov configuration has shown hydrodynamic signatures, namely flux vortex and negative resistance regions.

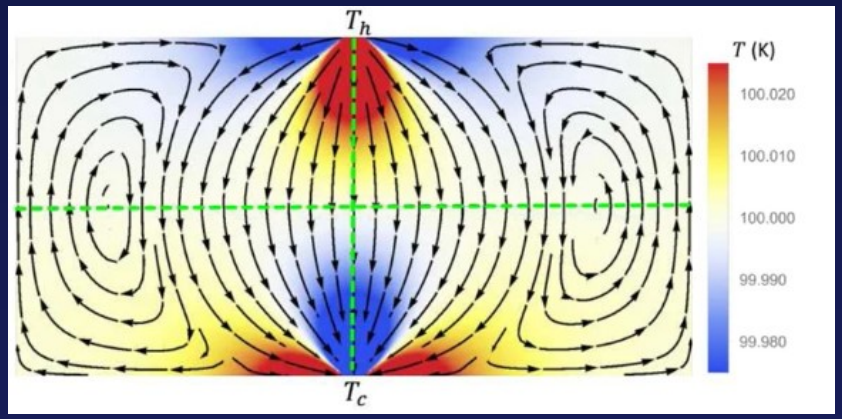

Reproduced from Shang et al., Sci. Rep. 10, 8272 (2020).

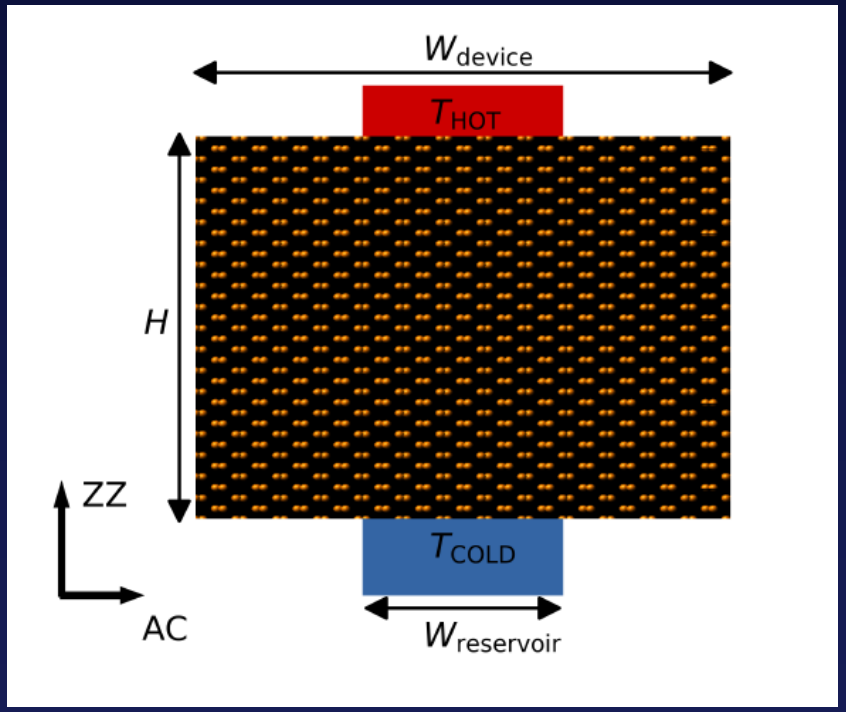

Sketch of a Levitov configuration with characteristic lengths H, $W_{reservoir}$ and W_{device} indicated. The transport axis, armchair (AC) and zigzag (ZZ), for phosphorene case are given as reference.

Levitov configuration and hydrodynamic signatures

- Levitov configuration has shown hydrodynamic signatures, namely flux vortex and negative resistance regions.

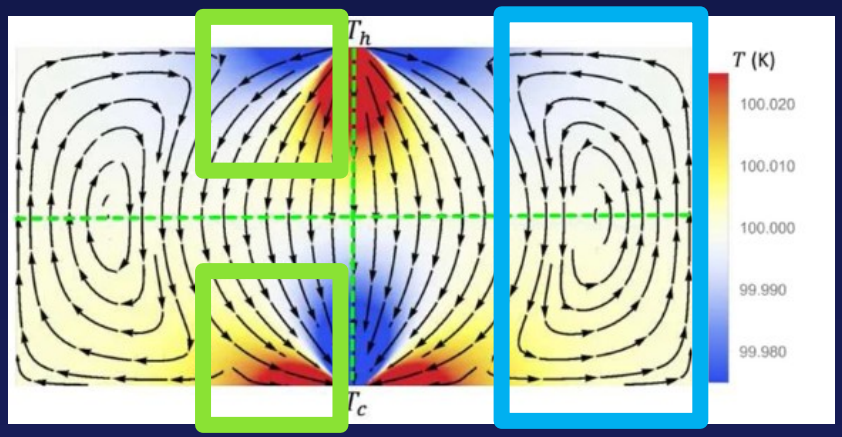

Reproduced from Shang et al., Sci. Rep. 10, 8272 (2020).

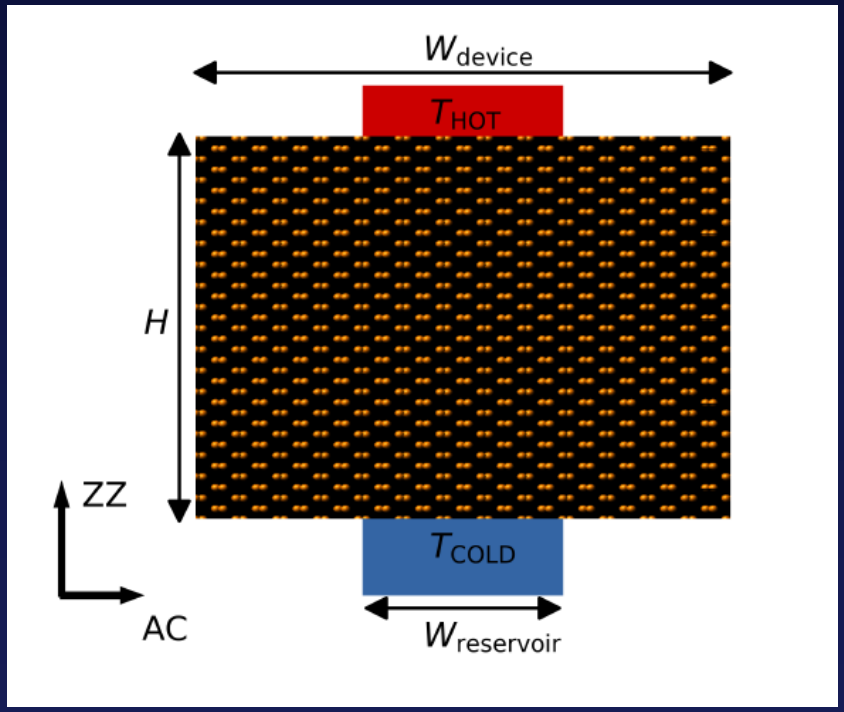

Sketch of a Levitov configuration with characteristic lengths H, $W_{reservoir}$ and W_{device} indicated. The transport axis, armchair (AC) and zigzag (ZZ), for phosphorene case are given as reference.

Levitov configuration and hydrodynamic signatures

- Levitov configuration has shown hydrodynamic signatures, namely flux vortex and negative resistance regions.
- Only studied through non-systematic approaches to the scattering, e.g. Callaway model.

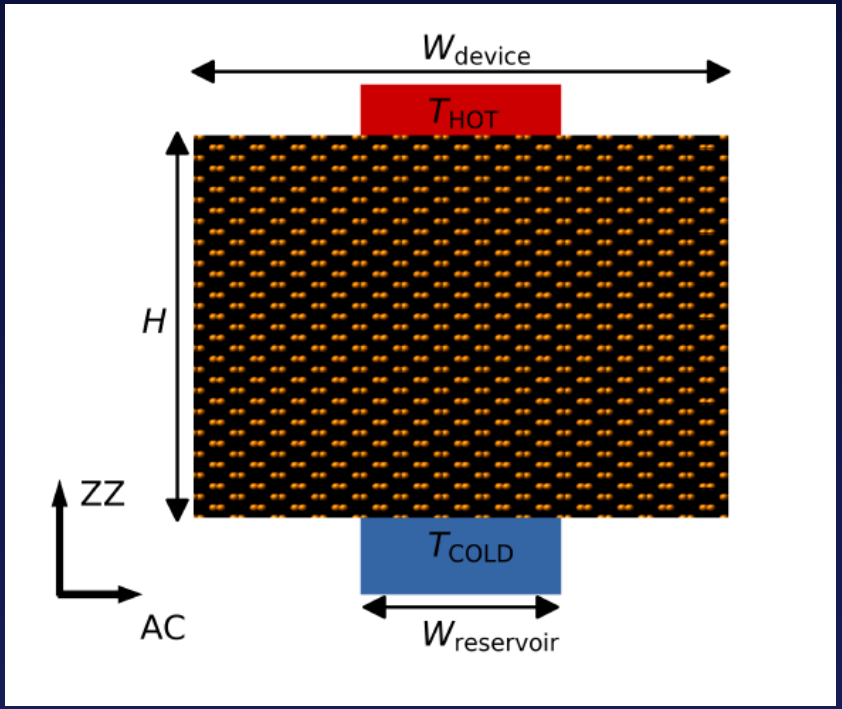

Sketch of a Levitov configuration with characteristic lengths H, $W_{reservoir}$ and W_{device} indicated. The transport axis, armchair (AC) and zigzag (ZZ), for phosphorene case are given as reference.

Quasiballistic devices (H< λ)

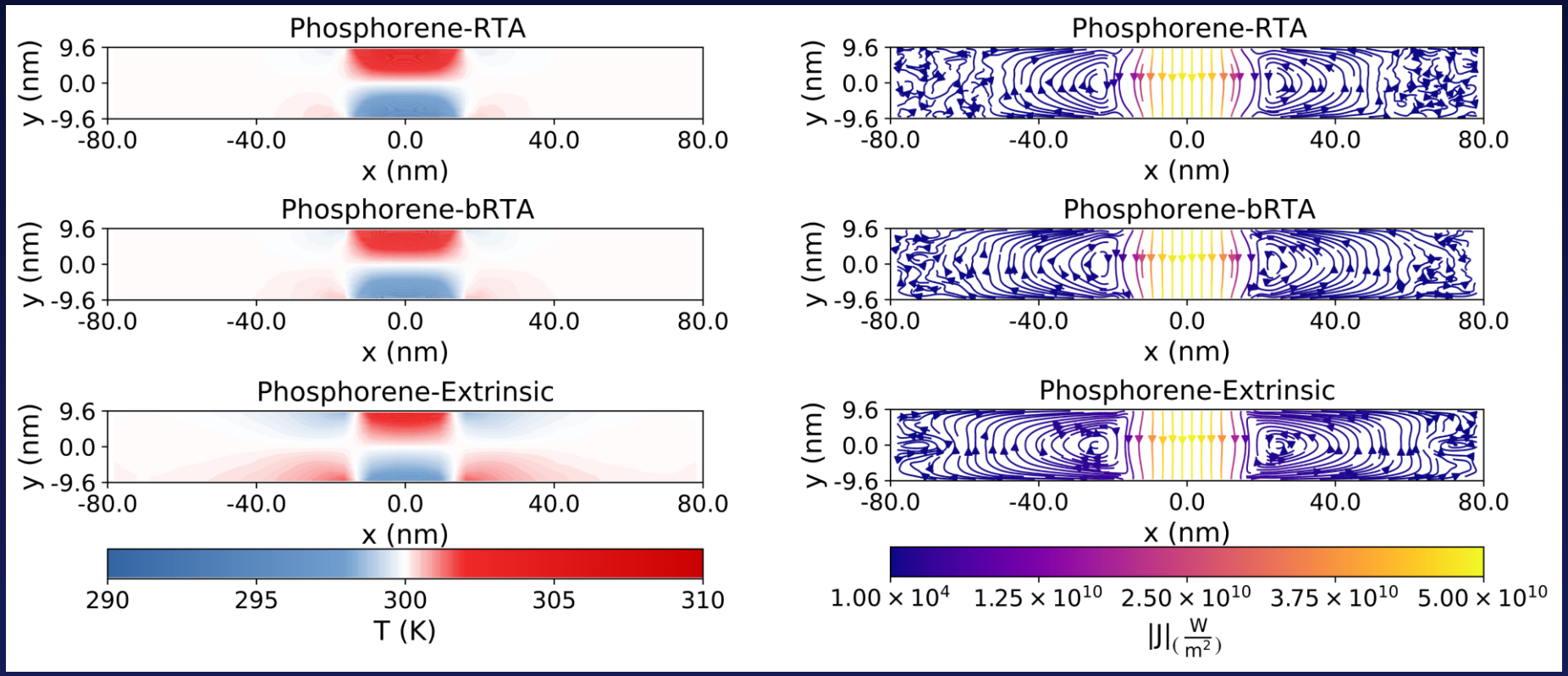

Thermal profiles (left) and heat fluxes (right) for a ballistic phosphorene-based Levitov.

Quasiballistic devices (H< λ)

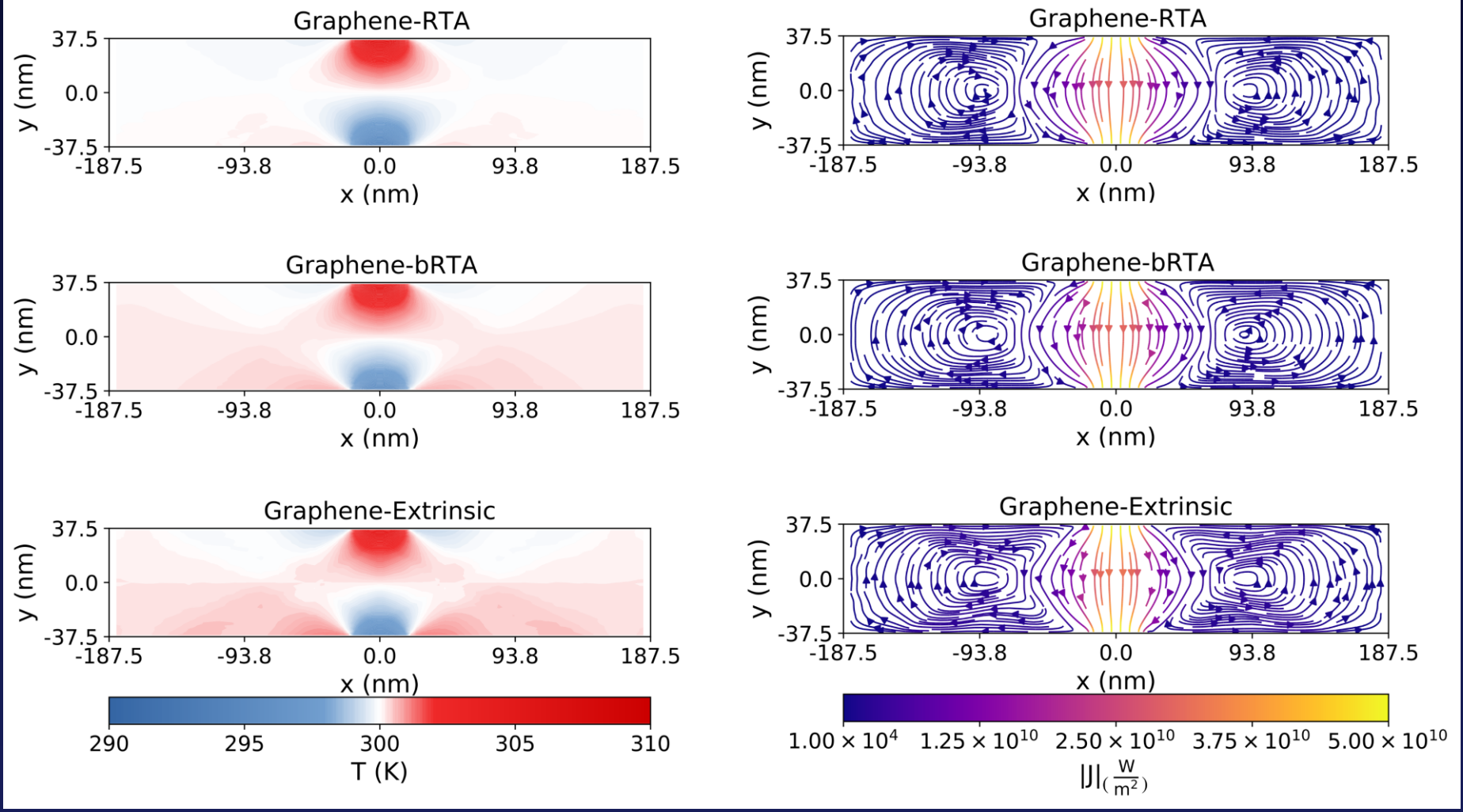

Thermal profiles (left) and heat fluxes (right) for a ballistic graphene-based Levitov.

Quasiballistic devices (H< λ)

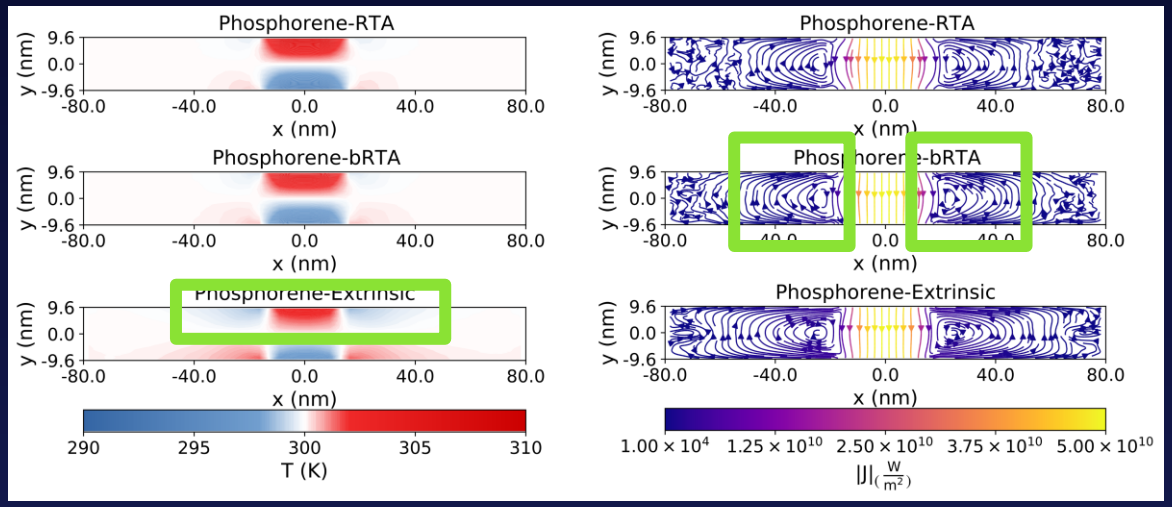

- Temperature steps near reservoirs (Ballistic feature).
- RTA and bRTA fluxes are similar (boundary scattering predominance; Ballistic feature).
- Heat flux vortices (Hydrodynamic feature).
- Negative resistance zone at the sides of the reservoirs

Quasiballistic devices (H< λ)

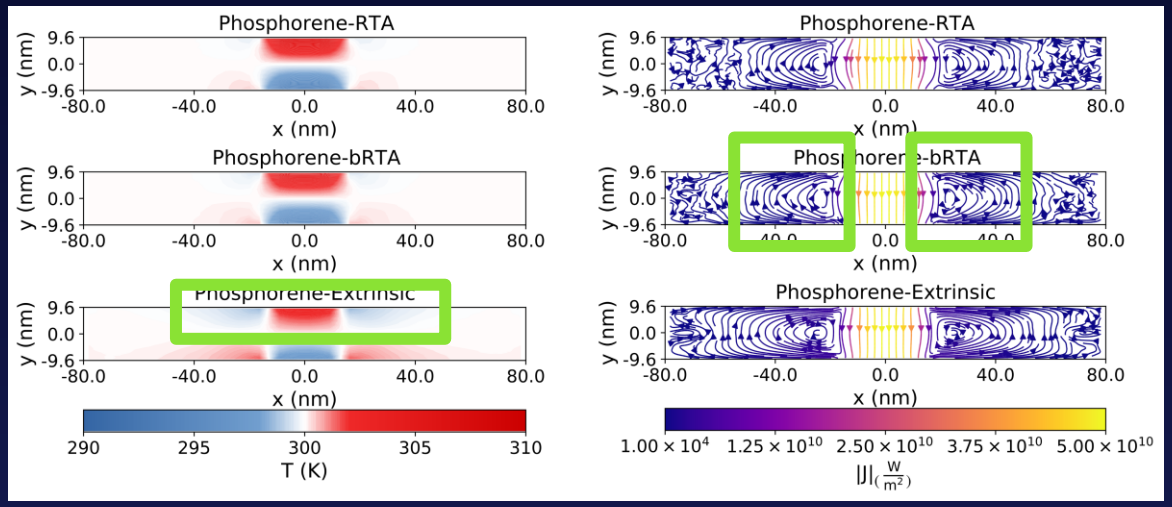

- Temperature steps near reservoirs (Ballistic feature).
- RTA and bRTA fluxes are similar (boundary scattering predominance; Ballistic feature).
- Heat flux vortices (Hydrodynamic feature).
- Negative resistance zone at the sides of the reservoirs
- EXTRINSIC HAS VORTICES, i.e. boundary scattering is the origin.

Quasiballistic devices ($H < \lambda$)

We are quasiballistic. So, does scattering treatment matter?

Quasiballistic devices (H< λ)

We are ballistic. So, does scattering treatment matter?

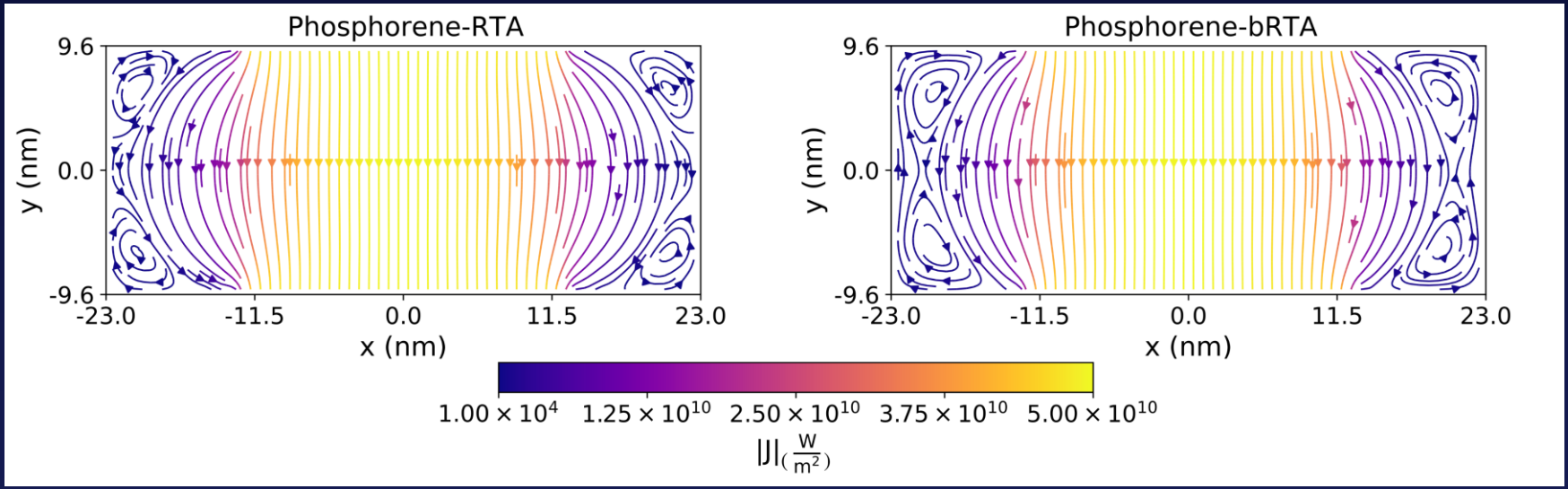

The RTA and bRTA heat flux for a limiting Levitov phosphorene-based configuration

Quasiballistic devices (H< λ)

We are ballistic. So, does scattering treatment matter?

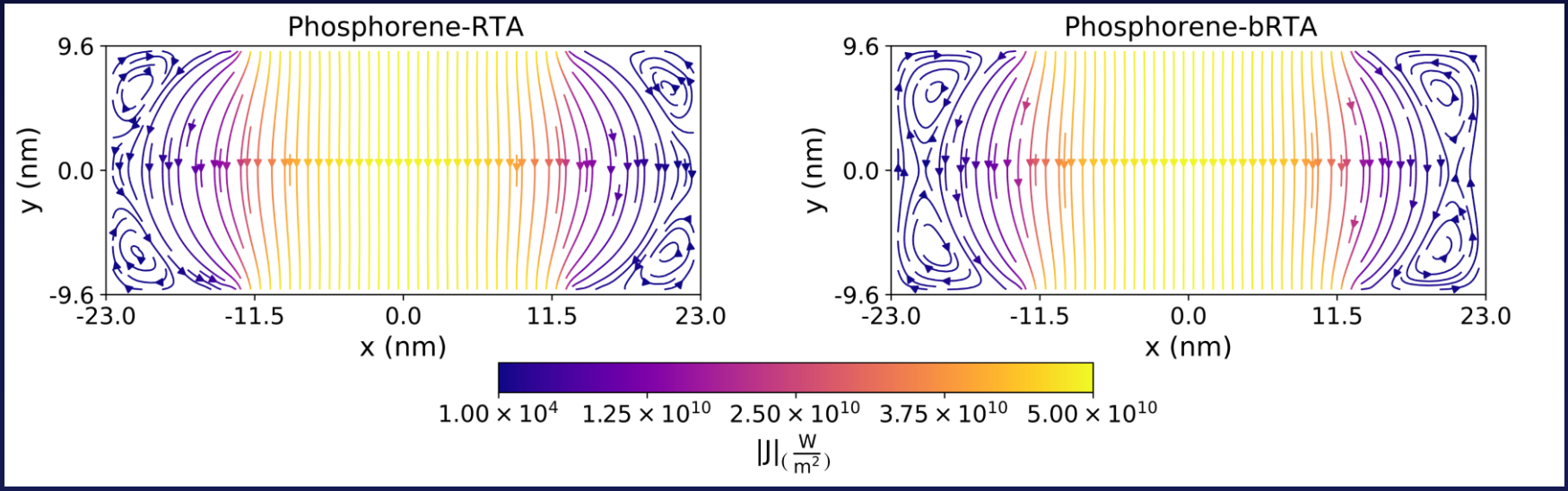

The RTA and bRTA heat flux for a limiting Levitov phosphorene-based configuration

<u>YES</u>, the RTA can lead to the wrong number of vortices in limiting cases. Rooted on RTA overhindering nature.

Quasiballistic devices (H< λ): Vortex formation

We look at vortex formation to check the mechanism originating them

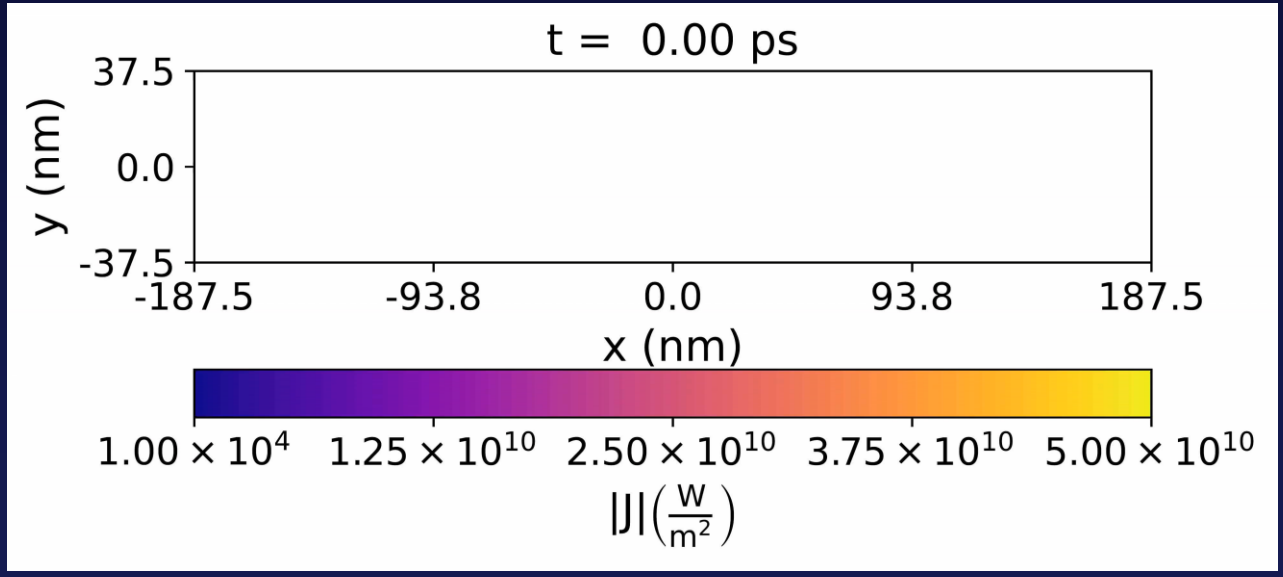

bRTA heat flux time evolution for a graphene-based Levitov configuration with $W_{device} = 3.75\ \mu m$.

Quasiballistic devices (H< λ): Vortex formation

We look at vortex formation to check the mechanism originating them

<u>Vortices form before phonons can arrive the vertical walls</u>

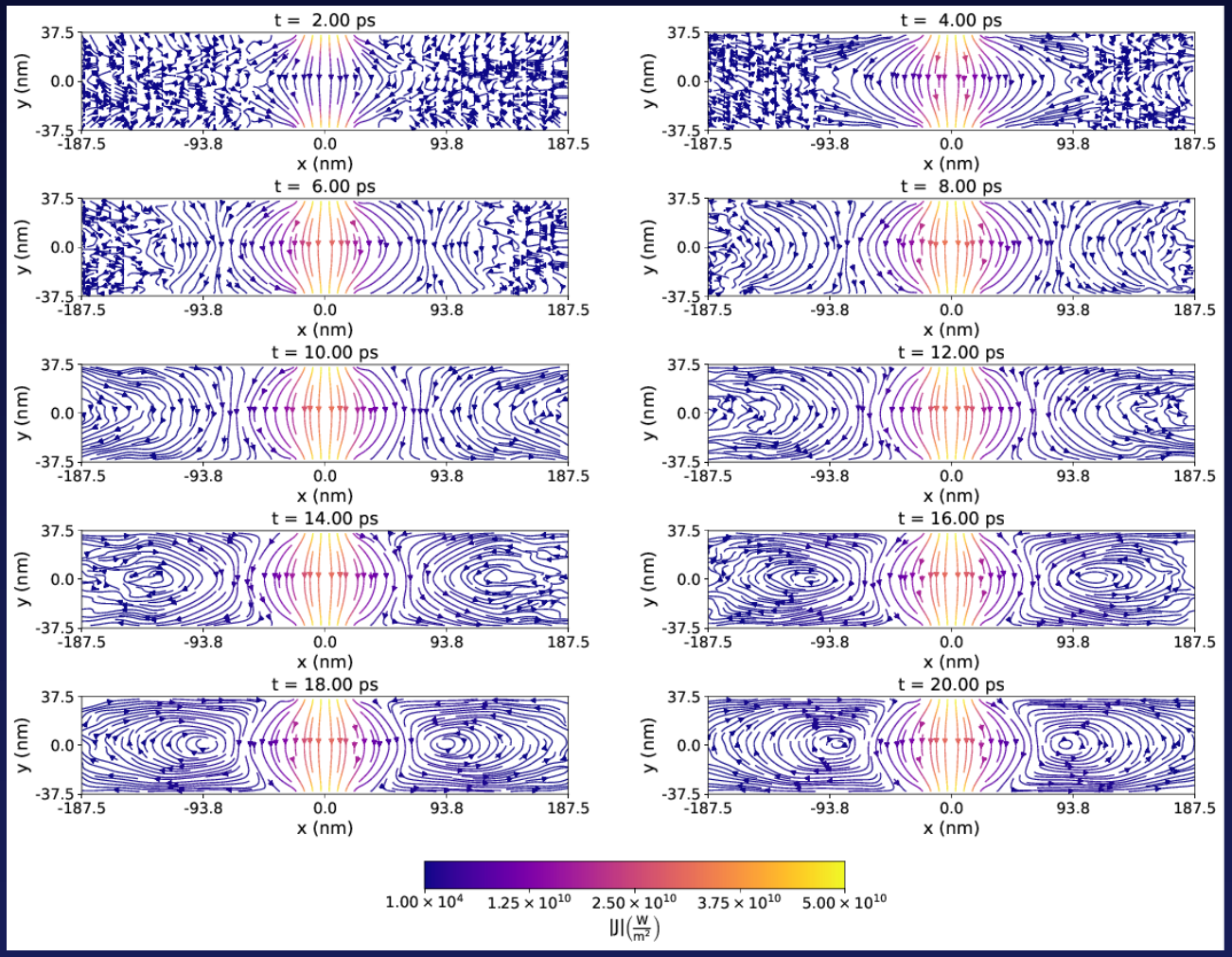

bRTA heat flux at different times for a graphene-based Levitov configuration with $W_{device} = 3.75\ \mu m$.

Quasiballistic devices (H< λ): Vortex formation

We look at vortex formation to check the mechanism originating them

<u>Vortices form before phonons can arrive the vertical walls</u>

Boundary scattering with horizontal walls is the leading mechanism behind vortices.

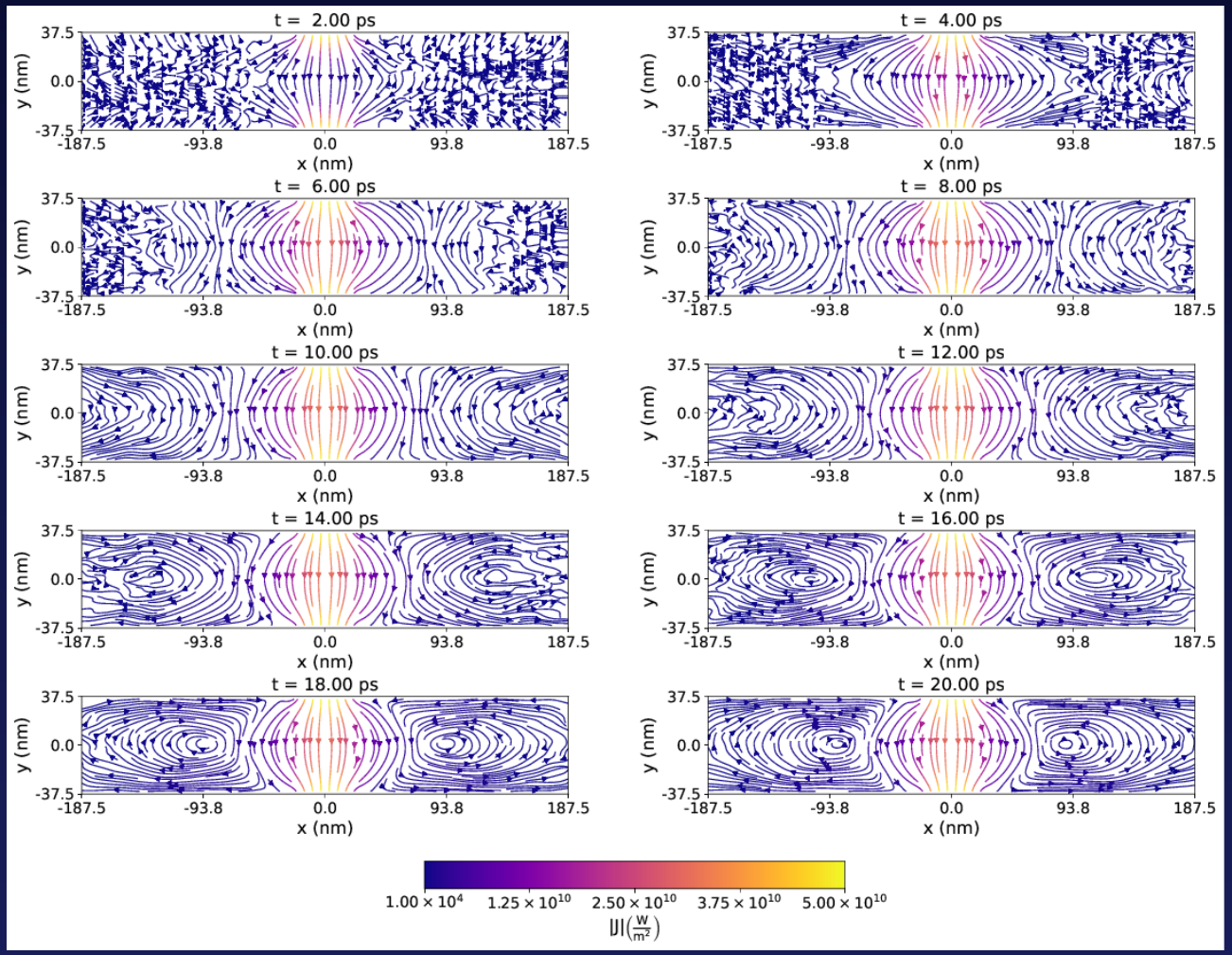

bRTA heat flux at different times for a graphene-based Levitov configuration with $W_{device} = 3.75\ \mu m$.

Conclusions

Conclusions

- BTE-Barna extends the capabilities of almaBTE to work with complex 2D-based systems. It can be freely downloaded from:

https://github.com/sousaw/BTE-Barna

- It enables the study of hydrodynamic features in real space for 2D materials-based devices.

Acknowledgements

Acknowledgements

- Ministerio de Educación, Cultura y Deportes
  - FPU2016/02565

- Ministerio de Universidades:
  - EST19/00655

- MINECO/FEDER
  - TEC2015-67462-C2-1-R

- MICIU/AEI/FEDER
  - RTI2018-097876-B-C21